Whole Heliosphere and Planetary Interactions (WHPI): The Big Picture on Solar Cycle Minima

Sarah Elizabeth Gibson[1], Robert Colby Allen[2], Giuliana de Toma[1], Barbara A. Emery[3], Federico Gasperini[4], Ian Hewins[1], Mary K. Hudson[5], Liying Qian[1], and Barbara J. Thompson[6]

[1]National Center for Atmospheric Research (UCAR)
[2]Johns Hopkins University Applied Physics Laboratory
[3]High Altitude Observatory
[4]Orion Space Solutions
[5]NCAR/HAO
[6]NASA Goddard SFC

April 4, 2023

Abstract

The Whole Heliosphere and Planetary Interactions (WHPI) is an international initiative to study the most recent solar minimum and its impact on the interconnected solar-heliospheric-planetary system by facilitating and encouraging interdisciplinary activities. Particular WHPI science foci include the global connected structure of the heliosphere and planetary space environments/atmospheres, the origins and impacts of high-speed solar wind streams, coronal mass ejections (CMEs) from Sun-to-Heliopause, and comparative solar minima. This is achieved through a series of coordinated observing campaigns, including Parker Solar Probe perihelia, and scientific virtual interactions including a dedicated workshop where observers and modelers gathered to discuss, compare, and combine research results. This introduction sets the scene for the WHPI interval, placing it into the context of prior initiatives and describing the overall evolution of the system between 2018-2020. Along with the accompanying articles, it presents a selection of key scientific results on the interconnected solar-heliospheric-planetary system at solar minimum.

Whole Heliosphere and Planetary Interactions (WHPI): The Big Picture on Solar Cycle Minima

Sarah E. Gibson[1], Robert C. Allen[2], Giuliana de Toma[1], Barbara Emery[1], Federico Gasperini[3], Ian Hewins[1,3], Mary Hudson[1], Liying Qian[1], and Barbara Thompson[4]

[1]High Altitude Observatory, National Center for Atmospheric Research, Boulder, CO 80305, USA
[2]Johns Hopkins University Applied Physics Laboratory, Laurel, MD, 20723, USA
[3]Orion Space Solutions, Louisville, CO 80027, USA
[4]NASA, Goddard Space Flight Center, Heliophysics Science Division, Greenbelt, MD 20771, USA

Key Points:

- The Whole Heliosphere and Planetary Interactions initiative studies the solar-heliospheric-planetary system's response to solar minimum.
- Solar minimum time periods provide an opportunity to characterize the baseline system and to trace events from "end to end".
- By comparing solar minima of multiple solar cycles, we gain insight into how the system changes over decadal times scales.

Corresponding author: Sarah Gibson, `sgibson@ucar.edu`

Abstract

The Whole Heliosphere and Planetary Interactions (WHPI) is an international initiative to study the most recent solar minimum and its impact on the interconnected solar-heliospheric-planetary system by facilitating and encouraging interdisciplinary activities. Particular WHPI science foci include the global connected structure of the heliosphere and planetary space environments/atmospheres, the origins and impacts of high-speed solar wind streams, coronal mass ejections (CMEs) from Sun-to-Heliopause, and comparative solar minima. This is achieved through a series of coordinated observing campaigns, including Parker Solar Probe perihelia, and scientific virtual interactions including a dedicated workshop where observers and modelers gathered to discuss, compare, and combine research results. This introduction sets the scene for the WHPI interval, placing it into the context of prior initiatives and describing the overall evolution of the system between 2018-2020. Along with the accompanying articles, it presents a selection of key scientific results on the interconnected solar-heliospheric-planetary system at solar minimum.

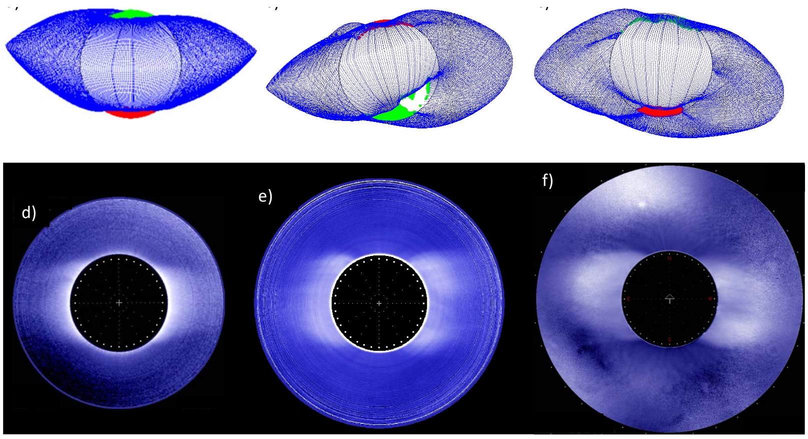

Figure 1. Three solar minima: 1996 Whole Sun Month (WSM); 2008-2009 Whole Heliosphere Interval (WHI); 2019-2020 Whole Heliosphere and Planetary Interactions (WHPI). a-c) National Solar Observatory Global Oscillations Network Group (NSO-GONG) line-of-sight coronal hole plots obtained from a potential field source surface extrapolation from solar surface magnetic fields (`https://gong.nso.edu/data/magmap/QR/bqg/`) for (left to right) January 31, 1996 (about six months before the official WSM solar rotation, and representative of that solar minimum's strongly dipolar structure); December 4, 2008 (WHI2 (Gibson et al., 2009); a rotation of relatively simple coronal structure); March 22, 2019 (Approximately midway through WHPI; a time of relatively simple coronal structure (see Section 4)). d-f) Mauna Loa Solar Observatory (MLSO) white light coronagraph images for the same three dates `https://mlso.hao.ucar.edu/mlso_data_calendar.php`).

1 Introduction

Why study solar minimum? Isn't it boring? After all, solar activity waxes and wanes with sunspot number, and, at solar minimum, it is definitely wane time (Hathaway, 2015). Solar flares and coronal mass ejections (CMEs) and their associated space-weather impacts at the Earth and other planets reach their lowest ebb during solar sunspot minimum (Temmer, 2021). However, as this paper and referenced articles demonstrate, there is more to the Sun and its impact on the heliosphere and planets than the activity associated with sunspots. In addition, when things are simple, end-to-end connections are easier to trace. Finally, solar minimum presents an opportunity to characterize the baseline, or ground state, of the heliosphere and planetary environments, and to consider how this baseline changes from one solar cycle to the next.

The Whole Heliosphere and Planetary Interactions (WHPI) is an international initiative focused on the solar minimum period. WHPI follows two similar initiatives during previous solar minima. Each initiative has expanded in scope, from Sun-to-solar-wind science during the Whole Sun Month (WSM) of 1996, to Sun-to-solar-wind-to-geospace science during the Whole Heliosphere Intervals (WHI) of 2008-2009, to the studies of Sun-to-solar-wind-to-planetary interactions of WHPI in 2018-2020 (Figure 1). The success of these efforts relies on a broad participation of scientists worldwide and across disciplines, and with each iteration such participation has increased. The WHPI mailing list currently has 777 subscriptors and continues to grow, and the September 2021 WHPI workshop had over 200 registered participants from 30 countries, resulting in a broad variety of talks and posters and a vibrant community discussion that has informed and enriched this introductory paper.

The structure of this paper is as follows. Section 2 describes the interconnected system at solar minimum, from Sun to solar wind, and from Sun to solar wind to planets. Section 3 provides a brief history of the "whole" intervals, for which WHPI is the third data point, and discusses WHPI in the context of these and other solar minima. Section 4 steps through "a year in the life" of the WHPI solar minimum, demonstrating the fascinating science that these quiet time periods inspire. Finally, Section 5 presents our conclusions.

2 The Interconnected System at Solar Minimum

2.1 From Sun to Solar Wind

The heliosphere is filled with a solar wind that originates from and is structured by the Sun's magnetic fields. Most of our observations of the solar wind are obtained *in situ*, by sending a satellite into space and measuring solar wind properties locally. A significant boost to our understanding came when the Ulysses satellite (McComas et al., 1998, 2003) moved out of the ecliptic, firmly establishing that fast wind emerges from the dark coronal holes seen in solar observations (Figure 2b). At solar minimum, this fast wind is primarily from the well-established polar coronal holes (Figure 2a), and slow wind is centered on the equator where bright coronal streamers trace out the predominantly dipolar magnetic structure of the Sun's corona (Figure 1).

This is somewhat of an over-simplification: we will discuss the importance of low-latitude high-speed solar wind streams at solar minimum and during the declining phase leading up to solar minimum, and, as we will see in Section 3, some solar minima have more magnetic complexity than others. Nevertheless, it is certainly true that solar minima are less complex than solar maxima, which are characterized by mixed fast and slow solar-wind speed at all latitudes. Solar maxima are also more dynamic than solar minima, with multiple coronal mass ejections expanding out through the heliosphere on any given day. Interestingly, the increase of structure and dynamics in the heliosphere at maximum results in a suppression of galactic cosmic rays (GCRs) so that when sunspot number is high at the Sun, GCR levels in the heliosphere are low, while at solar minimum, GCR levels reach their maximum level (Potgieter, 2013; Poopakun et al., 2022).

The source regions of high-speed solar wind observed at the Earth are generally low-latitude (near-equatorial) coronal holes – which can occur even during solar mini-

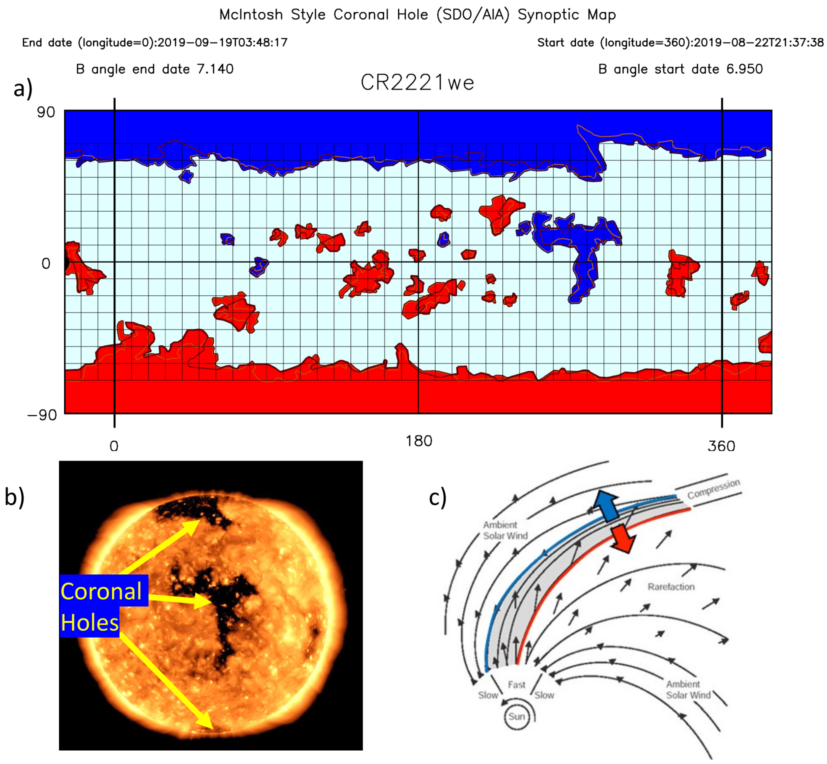

Figure 2. Fast solar wind originates in magnetically-open coronal holes. a) Example of a solar synoptic (latitude vs longitude) McIntosh Archive style map (Gibson et al., 2017; Webb et al., 2018, `https://www2.hao.ucar.edu/mcintosh-archive`) developed for WHPI (Hewins, Gibson, Webb, et al., 2023 under review, for this collection). The map is from Carrington Rotation 2221, August 22 - September 19, 2019. Coronal holes are represented in blue (positive magnetic polarity) and red (negative magnetic polarity). The polar coronal holes extend across all longitudes at both poles, but lower latitude (equatorial) coronal holes also exist. The large T-shaped blue (positive polarity) coronal hole centered around 270° solar longitude is discussed in further detail in Section 4.3, and seen in b) EUV image (SDO/AIA; March 29, 2019). c) Schematic diagram (view from heliographic pole) of fast wind catching up with slow wind and creating a Stream Interaction Region (SIR; adapted from Pizzo (1978) and Jian et al. (2006)).

mum (Figure 2b). Global magnetic models that use observations of the magnetic field at the Sun's surface, or photosphere, as a boundary condition (e.g., Figure 1a-c) find that when magnetic field lines extending out from the core of coronal holes line up with a spacecraft that samples the solar wind *in situ*, they are the source of high-speed solar wind streams (Wang & Sheeley, 1990, 1991; Riley et al., 2019). As the Sun rotates, solar wind emerges in a spiral pattern (Figure 2c), and if fast wind from a low-latitude coronal hole catches up with slower wind in front of it, it can create a Stream Interaction Regions (SIR; (Pizzo, 1978)) of compressed magnetized plasma that can drive space weather. If the low-latitude coronal hole lives for multiple solar rotations, these become Corotating Interaction Regions (CIRs) and act as periodic drivers of the solar wind and planetary environments. Since most of the interaction regions described in this paper persist, the terms SIR, CIR, and high-speed solar wind stream will essentially be used interchangeably for the remainder of the paper.

2.2 From Sun to Solar Wind to Planets

Because of the prevalence of long-lived low-latitude coronal holes during the months leading up to solar minima (Hewins et al., 2020), SIRs are the dominant drivers of space weather at the Earth and other planets during low-solar-activity times (Tsurutani et al., 2006). Although they do not have the coherent, rotating magnetic structure of CMEs, SIRs are otherwise quite similar in that they are characterized by a jump in dynamic pressure along with increased velocity and magnetic field strength (Bingham et al., 2018). As a consequence, SIRs compress planetary bowshocks and magnetopauses (Borovsky & Denton, 2006).

In general, the sensitivity of planetary magnetospheres to such solar wind forcing varies from planet to planet (Bagenal, 2013) (and from star to star; see Varela et al. (2022)). In the solar system, Jupiter and Saturn's magnetic fields are much stronger than Earth's, and their magnetospheres are only weakly driven by the solar wind as they are dominated by internal forcing (Vasyliunas, 1983; McComas & Bagenal, 2007; Delamere & Bagenal, 2010, 2013) with primary sources of plasma to their magnetospheres coming from their satellites, Io and Enceladus (Delamere et al., 2007; Blanc et al., 2015; Allen et al., 2018; Bagenal & Dols, 2020). The nature of Uranus and Neptune's magnetospheres are less well-understood, but Gershman and DiBraccio (2020) argued that, due to their highly tilted rotation relative to their magnetic dipoles, solar-wind driving may play an important role in convection within their magnetospheres (Vasyliunas, 1986). In contrast, there is no question about the Earth's magnetospheric response to external processes, as reconnection in the magnetotail drives auroral precipitation at the poles and plasma convection at Earth's high latitudes (Dungey, 1961). Mercury is also dominated by external forcing, not surprisingly due to its extreme proximity to the Sun. For the most extreme CME events, its dayside magnetosphere disappears, leaving Mercury exposed to the solar wind (Slavin et al., 2019; Winslow et al., 2020). This is always true at Mars, which has an induced magnetosphere and is only weakly shielded from impacts by solar and interplanetary disturbances (Jakosky et al., 2015; Lee et al., 2017). Venus also has an induced magnetosphere and auroral processes that depend upon solar wind pressure (Luhmann et al., 2007, 2008; Edberg et al., 2011).

The effects of solar wind forcing on a planetary magnetosphere and atmosphere has been most comprehensively observed at the Earth, where both CMEs and SIRs drive geomagnetic storms (Borovsky & Denton, 2006). These in turn lead to enhanced wave activity, auroral and radiation belt particle precipitation (Bingham et al., 2018; Millan & Thorne, 2007), which leads to an increase in ionospheric temperature, plasma density, and ion upflows and outflows (Wang et al., 2011; Ogawa et al., 2019) and also impacts Earth's neutral atmosphere (thermosphere) thermal structure, density and composition (Solomon et al., 2012; Younas et al., 2022, a paper in this collection). When there is a CIR surviving for multiple rotations, the result is periodic forcing of the Earth's space environment and upper atmosphere. Such periodicities are observed in a range of indices including geomagnetic indices, total electron content (ionosphere), neutral density (thermosphere), and energetic electrons (radiation belt) (Gibson et al., 2010; Emery et al., 2009; Lei et al., 2011). We will return to this in Section 4.

As we will also discuss further in Section 4, SIRs in the solar wind have been observed by the Mars Atmosphere and Volatile EvolutioN (MAVEN) satellite in orbit around Mars. In the Martian atmosphere, it can be difficult to separate out the effects of periodic particulate (solar wind) forcing vs radiative forcing. The most common periodic radiative forcing comes from the Sun's 27-day rotation which arises from any large long-lived solar active region (or indeed any long-lived solar feature) (J. Lean, 1997). Hughes et al. (2022) compared MAVEN solar irradiance observations with measurements of Mars thermospheric densities, and found clear correlations, especially at high altitudes. In a related study, Gasperini et al. (2023, a paper in this collection) compared the response of Mars' and Earth's thermospheres to EUV variation at solar minimum vs solar maximum and found greatly increased response of the middle thermospheric densities to solar rotation during the time of reduced EUV forcing at solar minimum for both planets. This may be explained by a reduction in adiabatic cooling due to rising motions in global circulation at low and middle terrestrial latitudes during solar minimum (Bougher et al., 2000, 2015).

Further subtleties arise at Mars because different wavelengths of light drive different reactions at different heights in the atmosphere (Thiemann et al., 2018). In particular, EUV wavelengths drive a direct effect involving local heating that has greatest impact in the upper Martian atmosphere, while infrared (IR) irradiance, which varies with variations in Mars' orbital distance from the Sun, has an indirect effect through upward coupling from the cooled lower-middle atmosphere. As a result, for high altitudes in the Mars atmosphere at solar maximum, the EUV effect may dominate compared to the solar-cycle-independent orbital (IR) effect, while at solar minimum, the EUV effect plays a relatively minor role (Fang et al., 2022).

3 Comparative Solar Minima

3.1 A Brief History of the "Whole Intervals"

The first of the "Whole" minimum campaigns was the Whole Sun Month (WSM) which occurred during a "classic" solar minimum in 1996. The solar corona was characterized by a global dipole field with streamer belts at the equator and large coronal holes at both poles (Figure 1a,d) as well as one equatorial coronal hole extension known as the Elephant's Trunk, which was the source of a fast wind stream impacting the Earth. The papers coming out of WSM marked the opening of the floodgates of Sun/solar wind scientific collaborations inspired by the SOHO satellite (Torsti, Anttila, & Sahla, 1999; Fludra et al., 1999; Linker et al., 1999; Del Zanna & Bromage, 1999; Dobrzycka et al., 1999; Biesecker et al., 1999; Warren & Hassler, 1999; Riley et al., 1999; Guhathakurta et al., 1999; Clegg et al., 1999; Breen et al., 1999; Panasyuk, 1999; Galvin & Kohl, 1999; Posner et al., 1999; Alexander, 1999; Gopalswamy et al., 1999; Torsti, Kocharov, et al., 1999; Zidowitz, 1999; Zhao et al., 1999; Gibson et al., 1999; Strachan et al., 1999; Gibson et al., 1999; Strachan et al., 2000; Bromage et al., 2000; Riley et al., 2001; Frazin & Janzen, 2002; Guhathakurta et al., 2006; Lionello et al., 2009).

This first WSM initiative focused on just one solar rotation (August 10-September 8, 1996) during solar minimum, but was followed by two related campaigns in 1998 (WSM2) and 1999 (WSM3) (Eiscat et al., 2000; Moran et al., 2000; Breen et al., 2000; Gibson et al., 2002; Gibson, 2001; Del Zanna et al., 2002; Ko et al., 2005).

The next solar minimum saw the organization of the Whole Heliosphere Interval (WHI) in 2008. The scope was expanded from Sun to Earth, and dozens of solar, heliospheric, and geospace instruments were involved. The WHI minimum was surprisingly different than WSM and other prior space-age solar minima. Despite an extremely low number of sunspots, there was more structure in the corona and heliosphere, with multiple broad low-latitude coronal holes and periodic forcing of the earth's space environment by high speed streams in 2008 (WHI1: CR2068, March 20 - April 16, 2008). The WHI minimum continued to evolve and become even quieter in 2009, becoming longer and deeper than any space-age solar minimum witnessed prior to it (WHI2/WHI3: CR2078/ CR2085, December 17, 2008 - January 12, 2009/ June 26 – July 22, 2009). The high-speed streams faded out, resulting in extreme depletion of radiation belt electrons at Earth (X. Li et al., 2013), as well as weak interplanetary magnetic field and record high levels of galactic cosmic rays (Mewaldt et al., 2010; Schwadron et al., 2018). However, the Sun's corona never became as predominantly dipolar as in 1996 (Figure 1), possibly because the polar magnetic fields in 2009 were significantly weaker than in 1996.

WHI science was rich, with analyses continuing for years after the original campaign time periods (Woods et al., 2009; Chamberlin et al., 2009; Bisi et al., 2009; Gibson et al., 2009; Bisi et al., 2010; Verkhoglyadova et al., 2011; Bisi et al., 2011; Gibson et al., 2011; Thompson et al., 2011; Webb et al., 2011; Muller et al., 2011; Welsch et al., 2011; White et al., 2011; Petrie et al., 2011; de Toma, 2011; Nitta, 2011; Cremades et al., 2011; Altrock, 2011; Vásquez et al., 2011; Benito et al., 2022; Echer et al., 2011; Lepping et al., 2011; Riley et al., 2011; Zhao & Fisk, 2011; Emery et al., 2011; Lei et al., 2011; Araujo-Pradere et al., 2011; Wang et al., 2011, 2011; Haberreiter, 2011; Jackman & Arridge, 2011; Wiltberger et al., 2012; Hudson et al., 2012; Lopez et al., 2012; Bruntz et al., 2012; Solomon et al., 2012; Z. Li et al., 2014; J. L. Lean et al., 2014; Lin & Chen, 2015; Wiltberger et al., 2017; Candido et al., 2018; Chadney et al., 2022).

The third iteration was the Whole Heliosphere and Planetary Interactions (WHPI). Based on lessons learned from WSM and WHI, the interval was not confined to a few solar rotations, but covered the period from late 2018 through early 2020. The level of participation increased with its expanded scope encompassing Sun to solar wind to planetary magnetospheres and atmospheres. The articles accompanying this introduction (Hudson et al., 2021; Lloveras et al., 2022; Riley et al., 2022; Gasperini et al., 2023; Luhmann et al., 2022; Younas et al., 2022; Palmerio et al., 2022; Bregou et al., 2022; Mlynczak et al., 2022; Varela et al., 2022; Badman et al., 2023; Hewins, Gibson, Webb, et al., 2023 under review; Allen et al., 2023 under review) represent the beginnings of analyses that are likely to continue for years to come.

3.2 Comparative Solar Minima

At first glance, considering Figure 1, it appears that the solar magnetic structure of WHPI was a bit more like WSM than WHI, in that it had a more dipole-type structure with coronal holes centered on the poles. On the other hand, as discussed in Hewins, Gibson, Webb, et al. (2023 under review, a paper in this collection), the extended WHPI period had significant and persistent low-latitude coronal holes that disrupted this simple morphology, similar to what was observed during WHI. As we will discuss further in Section 4, the white light corona during WHPI was not always as dipolar as Figure 1 c). The low-latitude coronal holes were least prevalent in late March 2019 when the observations shown in Figure 1c) were taken, so that it represents the simplest, but not necessarily the typical structure during the WHPI extended interval.

Figure 3 shows the dipole vs quadrupole components of the photospheric magnetic field, showing that the dipole component was strongest during WSM, weakest during WHI, and in the middle during WHPI. This is consistent with the results of Riley et al. (2022, a paper in this collection) who found similar trends in the solar polar magnetic field, which is controlled by the strength of the dipole term. The overall coronal magnetic morphology of closed vs open field is impacted by the ratio of this dipole term relative to higher-

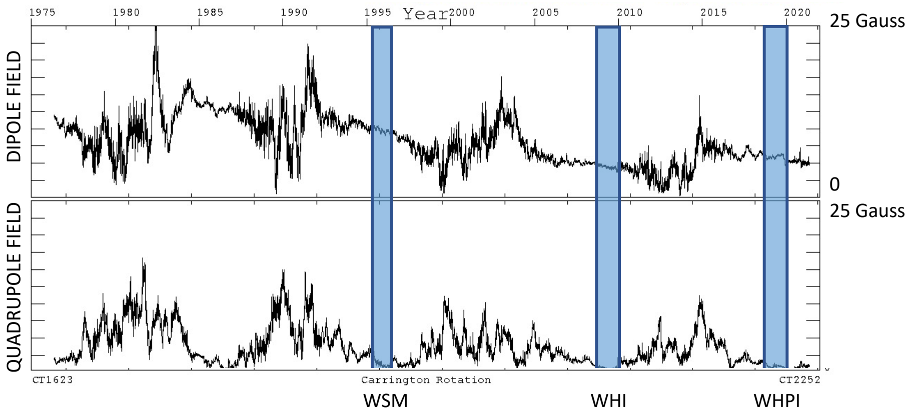

Figure 3. Dipole (top) and quadrupole (bottom) components of the solar photospheric magnetic field, as determined from observations obtained by Stanford's Wilcox Solar Observatory `http://wso.stanford.edu/gifs/Multipole.gif`. The three intervals, WSM, WHI, and WHPI are indicated by the shaded blue rectangles. From this it is clear that the dipolar field was strongest for WSM and weakest for WHI, with WHPI lying in between, but that the quadrupolar field was similar for all three.

order multipole fields. Figure 3 illustrates that the quadrupolar magnetic term is similar in all three intervals, but varies somewhat. In particular, it hits a low during March 2019. Thus, the global coronal magnetic structure as manifested in white-light observations (Figure 1) was predominantly dipolar during the shorter minimum of WSM, never attained that status during the extended minimum of WHI, and demonstrated both white-light dipolar structure and sustained low-latitude coronal holes during the extended WHPI minimum.

These differences of solar dipole strength and coronal magnetic morphology affect the nature of the solar wind near sunspot minimum. Riley et al. (2022) did a statistical comparison of the three solar minima and found, as was the case with the polar magnetic fields, that the WHPI solar wind properties lay in between those of WSM and WHI. Luhmann et al. (2022, a paper in this collection) determined the sources of solar wind velocity measured in the ecliptic from global coronal magnetic models and found that low-to-mid latitude open fields (as opposed to polar open fields) were the primary source of solar wind measured at the Earth, in particular during the extended minima of WHI and WHPI. Thus, to summarize, coronal magnetic field and solar wind observations indicate that WHPI was similar to WHI in its length and magnetic complexity, but demonstrated at least a "partial recovery" of solar dipole dominance and solar wind density and velocity. Thus, WSM > WHPI > WHI in terms of dipole dominance and solar wind properties at solar minimum.

However, the behavior at the Earth paints a somewhat different picture. Once anthropogenic effects (rising CO_2 levels, which cause a secular decrease in thermospheric temperatures) are taken into account, the Earth's upper atmosphere can be a sensitive measure of differences between solar minima. Using measurements of satellite drag, Emmert et al. (2010) found a decrease in thermospheric density ($\sim$ 30% at 400 km) and temperature during the WHI minimum relative to prior minima. (Solomon et al., 2011) conducted model simulations and found a $\sim$ 27% decrease of annual mean density changes at 400 km altitude from 1996 to 2008. Among this $\sim$ 27% decrease, $\sim$ 22%, $\sim$ 2.2%, and $\sim$ 3% were attributed to solar EUV decrease, geomagnetic activity change, and CO_2

increase, respectively. Mlynczak et al. (2022, a paper in this collection) measured a downward trend in thermospheric temperatures from 2002 to 2019 using measurements from the TIMED satellite. After accounting for anthropogenic CO_2 increase, they found temperatures at lower thermospheric altitudes ($10^{-4}hPa$, 105km) had dropped -14.37 K between 2002 and 2019 – and that the lower thermospheric temperatures in the 2019 minimum (WHPI) were $\sim 3K$ colder than the 2008-2009 minimum (WHI). Thus, in terms of thermospheric temperature, WSM < WHI < WHPI, with no sign of the "partial recovery" discussed by Riley et al. (2022).

Relatedly, Bregou et al. (2022, a paper in this collection) found a long-term (1980 to mid-2021) increase in inner zone radiation belt proton flux that they interpreted as a manifestation of the secular downtrend in F10.7 correlated with sunspot number known as the Centennial Gleissberg Cycle (Gleissberg, 1944; Feynman & Ruzmaikin, 2011). F10.7 serves as a proxy for solar EUV in the Bregou et al. study, with a decrease implying a reduced atmospheric (and ionospheric) scale height and reduced collisional drag at a fixed altitude, which is the primary loss mechanism for inner zone protons. Each solar minimum since 1980 has been followed by a maximum trapped proton flux which has shown a secular increase, modulated by the solar cycle, over the past 40 years. Thus, correlated with cooling in the thermosphere, the inner zone radiation belt proton flux has continued to increase with each successive minimum, so WSM < WHI < WHPI — again, no sign of a partial recovery and consistent with a response to the Sun's secular approach to the Gleissberg minimum in solar activity.

To explain the apparent discrepancy between the solar wind and planetary environmental trends, we consider the sometimes competing natures of radiative vs particulate forcing of planetary atmospheres. (Emmert et al., 2010) argued that the decrease in thermospheric densities and temperatures was a result of a decrease in EUV spectral irradiance from the WSM to the WHI solar minimum, and this was supported by the Solomon et al. (2011) modeling study, which found that irradiance changes between WSM and WHI were the dominant cause of the secular trend (relative to particulate and anthropogenic forcings). The case for decreased irradiance being the cause of the ongoing downward trend in thermospheric temperatures from WHI to WHPI is less clear: Using SORCE satellite data from 2003-2020, Woods et al. (2022) found no significant differences in integrated solar spectral irradiance between the two time periods – so, neither a "partial recovery" in irradiance nor a continuing decrease in integrated spectral solar irradiance. However, Mlynczak et al. (2022) argued that when one considered just the narrow Schumann-Runge Bands of solar ultraviolet radiation from 175 to 200 nm, a region responsible for heating of the lower thermosphere, there was a statistically significant decrease in SORCE-measured irradiance between the WHI and WHPI minima. Further modeling is needed to fully understand the causes of the decrease in thermospheric temperatures from WHI to WHPI.

4 Evolution of a Solar Minimum

WHPI spanned the entire solar minimum period between 2018 and 2020. For the purpose of coordinating targeted observations, we identified a few focus "campaign" time periods that took advantage of solar-heliosphere-planetary synergies. These included the solar eclipse in July 2019 – which was studied both for its solar structure (Lloveras et al., 2022, a paper in this collection) and for the Earth's thermospheric response to it as measured by the GOLD satellite (Aryal et al., 2020). They also included the Parker Solar Probe perihelion passage in January 2020 – which served as a template for community coordination and predictive targeting (Badman et al., 2023, a paper in this collection). Beyond that, we trusted to solar serendipity to provide interesting time periods for study, and we were not disappointed!

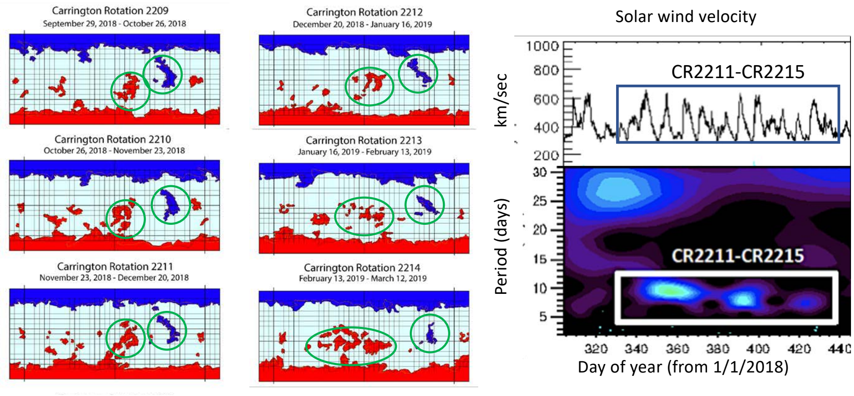

Figure 4. (left and middle columns) McIntosh Archive style Carrington maps (latitude vs. longitude; see Figure 2) for Carrington rotations 2209 through 2214 (September 21 2018 – March 5, 2019; note the ∼27-day solar rotations shown are "padded" on each side by a week of observations), showing long-lived low-latitude coronal holes of both polarities in the right half of maps (green circles). Adapted from Figure 10 of Hewins, Gibson, Webb, et al. (2023 under review). The effects of differential rotation (faster solar rotation at equator than higher latitudes) can be seen in the drift of the equatorial portion of both coronal holes to the right (the equator rotates prograde relative to the synoptic Carrington rate of 27.3 days; see discussion in Luhmann et al. (2022)). (right column) Solar wind at Earth vs time (top) and related wavelet (bottom) showing periodic solar wind 7-9 day forcing. Data from `https://omniweb.gsfc.nasa.gov/`.

4.1 September 2018 - March 2019 – Long-lived low-latitude coronal holes and periodic forcing

Even when solar activity was low, low-latitude coronal holes were present for a significantly long time period. In particular, two coronal holes of opposite polarity separated by approximately 90 degrees remained visible for several rotations (Figure 4 left and middle columns). As discussed in Hewins, Gibson, and Emery (2023 under review), both of these coronal holes resulted in repeating fast wind streams observed at Earth, Mars, and STEREO-A. This 7-9-day periodic solar-wind forcing, shown in Figure 4 right column, is not unlike that observed in the early phases of WSM (Gibson et al., 2010; Emery et al., 2009; Lei et al., 2011), with impact felt in the Earth's upper atmosphere as measured in neutral density by the Swarm-C satellites. Large effects were also registered in the ionosphere through ground-based GNSS total electron content (F. Gasperini, in preparation).

4.2 March 2019 - July 2019: Quiet with a burst of activity in the middle

The interval 2018 – 2020 was a long period of low solar sunspot number and solar magnetic activity, but it was briefly interrupted by a burst of old-cycle sunspot emergence and associated activity in April – June 2019 (Figure 5). This burst of activity resulted in multiple CMEs that erupted from a nest of active regions with impacts measured at both the Earth and Mars (E. Palmerio, private communication). Such events are excellent candidates for studying the evolution of CMEs in the solar wind as a function of distance from their solar origin (Witasse et al., 2017), as well as for considering the relative effects of CMEs vs SIRs on planetary space environments during times of

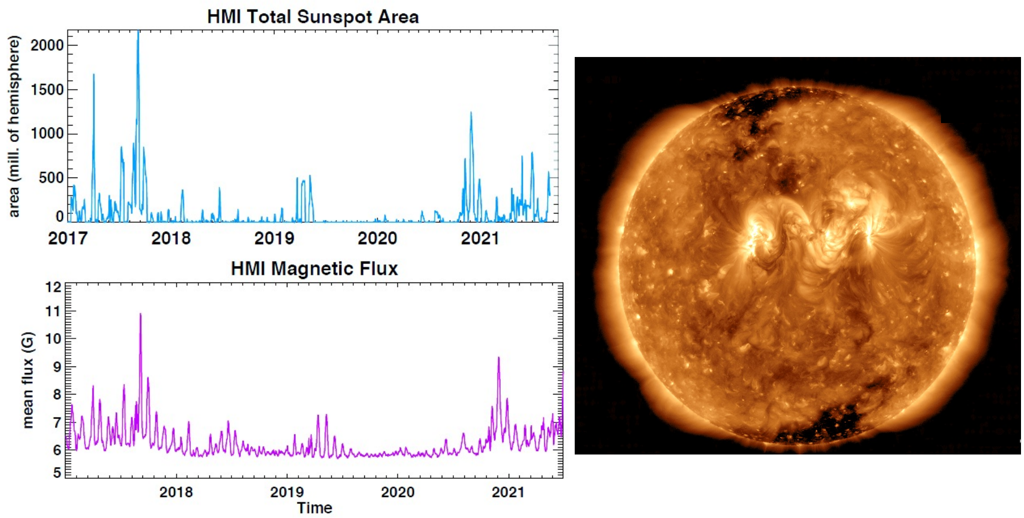

Figure 5. (left) Total sunspot area determined from Solar Dynamics Observatory (SDO) Helioseismic and Magnetic Imager (HMI) intensities (top) and associated magnetic flux (bottom), as a function of time during the WHPI solar minimum. (right) Nest of active regions during (May 12, 2019) which resulted in multiple CMEs detected throughout the solar system (SDO/AIA image, obtained via helioviewer.org)

.

relative heliospheric simplicity (Hudson et al., 2021, a paper in this collection). In an analysis of a series of solar transient events immediately prior to the WHPI time period (August 2018), Palmerio et al. (2022, a paper in this collection) was able to separate out the effects of two CMEs and a following high-speed stream by comparing observations at the Earth and Mars in the context of a global MHD model.

4.3 August - December, 2019: The persistance of "Mr. T"

The long-lived, low-latitude coronal holes of September 2018 - March, 2019 shown in Figure 4 had largely dissipated by April, 2019, in part due to differential rotation of these latitudinally-extended structures and resulting distortion and fragmentation (Hewins, Gibson, Webb, et al., 2023 under review). They were replaced by the active region nest of April-June 2019, which emerged and then decayed, to be replaced in turn by a new positive-polarity (blue) coronal hole that survived for approximately six months (Figure 6; see also Figure 2)).

This coronal hole was extremely geoeffective, perhaps due to its 'T' shape which meant that, near the equator, it was both wide in longitude (and so driving a longer-lasting fast wind stream in time), and tall in latitude (increasing the likelihood of the Earth being repeatedly hit by at least part of its stream). In early September, the sustained fast wind resulted in a radiation belt response that was the highest energy (hardest relativistic electron spectrum) observed in the last two years of the Van Allen Probes mission (Mauk et al., 2013). The radiation-belt response to the CIR lasted into October 2019 and was higher than the response seen during the CME events associated with the active region nest of May 2019 (Hudson et al., 2021).

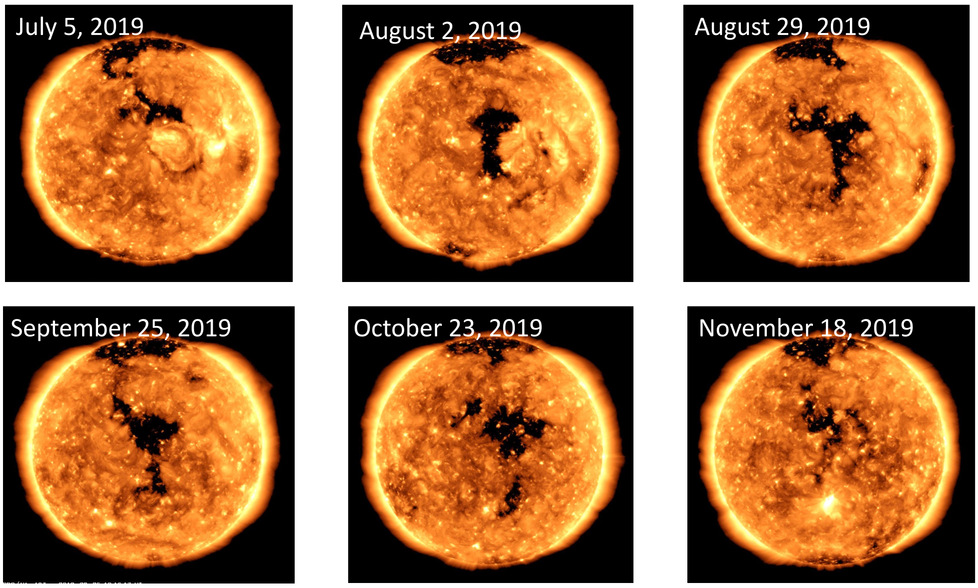

Figure 6. The 'Mr. T' long-lived coronal hole which recurred over six solar Carrington rotations. Shown here in 195 Å as observed by SDO/AIA.

The presence of this long-lived coronal hole at the Sun also overlapped with a time period when Parker Solar Probe was radially aligned with the STEREO-A spacecraft, allowing analyses of the evolution of the associated SIR and a study of energetic particle acceleration (Allen et al., 2021; Wijsen et al., 2021). Measurements of SIRs and CMEs at different longitudinal points in the solar system were also made possible via multi-spacecraft measurements. For a comprehensive overview of this coronal hole and its impacts throughout the heliosphere, see Allen et al. (2023 under review, a paper in this collection).

5 Conclusions

The science enabled by focusing on solar minimum is rich and rewarding. During WSM (1996) and WHI (2008-2009) we gained global understanding about the sources and impacts of solar wind, and new insight about how different solar minimum "quiet times" can be from one another. WHPI (2018-2020) is providing yet more insights into the whole heliospheric system. For example:

- The response to solar-wind and solar-irradiance forcings varies greatly from planet to planet. Analyses of the space-weather impacts that do occur is an excellent way to test our understanding of the coupled mechanisms at play.
- By coronal/solar wind forcing standards, WSM > WHPI > WHI, but radiation-belt and upper atmospheric observations show more of a monotonic secular trend, WSM < WHI < WHPI. This may be due to opposing trends in spectral irradiance vs. solar wind forcing over the past two minima. It illustrates the complexity of understanding system variability when multiple mechanisms – including anthropogenic ones – are involved.

- Multispacecraft/multipoint measurements throughout the heliosphere, varying both in distance and longitude, enable detailed analyses of the evolution of solar wind structures and their sources.

A final comment: with each minimum, observational and modeling capabilities have improved along with data-model interpretation schema. The international interdisciplinary initiatives of WSM, WHI, and WHPI act as catalysts for new analysis approaches and (importantly) play a role in building enduring cohorts of scientific collaborators across scientific disciplines. These efforts should be continued in future minima, as they play an important role in quantifying and understanding long-term changes in the Sun and their effects on the solar wind and planetary space environments and atmospheres.

6 Open Research

GONG magnetic field extrapolations are available at `https://gong.nso.edu/data/magmap/QR/bqg/`.

Mauna Loa Solar Observatory white light coronagraph images are available at `https://mlso.hao.ucar.edu/mlso_data_calendar.php`).

McIntosh archive maps presented in this paper are available through the NOAA National Centers for Environmental Information. doi:10.7289/V5765CCQ. The maps and supplemental reference/methodology materials are archived at `https://www.ngdc.noaa.gov/stp/space-weather/solar-data/solar-imagery/composites/synoptic-maps/mc-intosh/`. Further information on the use and application these data can be found at `https://www2.hao.ucar.edu/mcintosh-archive`.

Additional data appears from the Solar Dynamics Observatory Atmospheric Imaging Assembly (AIA) and Helioseismic and Magnetic Imager (HMI) as accessed through Helioviewer (`https://helioviewer.org/?movieId=hnTN5`). SDO data courtesy of NASA/SDO and the AIA, EVE, and HMI science teams.

Stanford Wilcox Solar Observatory dipole and quadrupole data may be obtained at `http://wso.stanford.edu/#Other`.

Solar wind data are available at `https://omniweb.gsfc.nasa.gov/`.

Acknowledgments
We are indebted to all the participants of the WHPI Workshop of September, 2021. We owe particular thanks to Saurav Aryal, Fran Bagenal, Joan Burkepile, Gina DiBraccio, Heather Elliott, Xiaohua Fang, Rachael Filwett, Dan Gershman, Lan Jian, Janet Kozyra, Christina Lee, Janet Luhmann, Carlos Martinis, Ryan McGranaghan, Marty Mlynczak, Erika Palmerio, Kledsai Poopakun, Nour Raouafi, Pete Riley, Yi-Ming Wang, Nicolas Wijsen, and Olivier Witasse. Funding for SEG, RCA, GdT, BE, IH, and LQ was provided by the NASA HSO Connect program. FG acknowledges support from NASA MDAP Grant No. 80NSSC21K1821. NCAR is a major facility sponsored by the NSF under Cooperative Agreement No. 1852977.

References

Alexander, D. (1999). Temperature structure of the quiet sun x ray corona. *Journal of Geophysical Research: Space Physics*, *104*(A5), 9701-9708. Retrieved from `https://agupubs.onlinelibrary.wiley.com/doi/abs/10.1029/1998JA900016` doi: https://doi.org/10.1029/1998JA900016
Allen, R. C., Gibson, S. E., Hewins, I. M., Vines, S. K., Qian, L., de Toma, G., ... Hill, M. (2023 under review). A Mosaic of the inner heliosphere: Three Car-

rington rotations during the Whole Heliosphere and Planetary Interactions Interval. . (under review [Paper 2023JA031361])

Allen, R. C., Ho, G. C., Mason, G. M., Li, G., Jian, L. K., Vines, S. K., ... Wiedenbeck, M. (2021, February). Radial Evolution of a CIR: Observations From a Nearly Radially Aligned Event Between Parker Solar Probe and STEREO A. , *48*(3), e91376. doi: 10.1029/2020GL091376

Allen, R. C., Mitchell, D. G., Paranicas, C. P., Hamilton, D. C., Clark, G., Rymer, A. M., ... Vandegriff, J. (2018, June). Internal Versus External Sources of Plasma at Saturn: Overview From Magnetospheric Imaging Investigation/Charge-Energy-Mass Spectrometer Data. *Journal of Geophysical Research (Space Physics)*, *123*(6), 4712-4727. doi: 10.1029/2018JA025262

Altrock, R. C. (2011, December). Coronal Fe XIV Emission During the Whole Heliosphere Interval Campaign. , *274*(1-2), 251-257. doi: 10.1007/s11207-011-9714-9

Araujo-Pradere, E. A., Redmon, R., Fedrizzi, M., Viereck, R., & Fuller-Rowell, T. J. (2011, December). Some Characteristics of the Ionospheric Behavior During the Solar Cycle 23 - 24 Minimum. , *274*(1-2), 439-456. doi: 10.1007/s11207-011-9728-3

Aryal, S., Evans, J. S., Correira, J., Burns, A. G., Wang, W., Solomon, S. C., ... Jee, G. (2020, September). First Global-Scale Synoptic Imaging of Solar Eclipse Effects in the Thermosphere. *Journal of Geophysical Research (Space Physics)*, *125*(9), e27789. doi: 10.1029/2020JA027789

Badman, S. T., Riley, P., Jones, S. I., Kim, T. K., Allen, R. C., Arge, C. N., ... Verniero, J. L. (2023). Prediction and verification of Parker Solar Probe solar wind sources. at 13.3 Rsun. . doi: 10.1029/2023JA031359

Bagenal, F. (2013). Planetary Magnetospheres. In T. D. Oswalt, L. M. French, & P. Kalas (Eds.), *Planets, stars and stellar systems. volume 3: Solar and stellar planetary systems* (p. 251). doi: 10.1007/978-94-007-5606-9_6

Bagenal, F., & Dols, V. (2020, May). The Space Environment of Io and Europa. *Journal of Geophysical Research (Space Physics)*, *125*(5), e27485. doi: 10.1029/2019JA027485

Benito, J., Kuo, P.-C., Widrig, K. E., Jagt, J. W. M., & Field, D. J. (2022, December). Cretaceous ornithurine supports a neognathous crown bird ancestor. , *612*(7938), 100-105. doi: 10.1038/s41586-022-05445-y

Biesecker, D. A., Thompson, B. J., Gibson, S. E., Flucra, A., Gopalswamy, N., Hoeksema, J. T., ... Strachan, L. (1999). Synoptic sun during the first whole sun month campaign: August 10 to september 8, 1996. *Journal of Geophysical Research: Space Physics*, *104*(A5), 9679-9689. Retrieved from `https://agupubs.onlinelibrary.wiley.com/doi/abs/10.1029/1998JA900056` doi: https://doi.org/10.1029/1998JA900056

Bingham, S. T., Mouikis, C. G., Kistler, L. M., Boyd, A. J., Paulson, K., Farrugia, C. J., ... Kletzing, C. (2018, December). The Outer Radiation Belt Response to the Storm Time Development of Seed Electrons and Chorus Wave Activity During CME and CIR Driven Storms. *Journal of Geophysical Research (Space Physics)*, *123*(12), 10,139-10,157. doi: 10.1029/2018JA025963

Bisi, M. M., Jackson, B. V., Buffington, A., Clover, J. M., Hick, P. P., & Tokumaru, M. (2009, May). Low-Resolution STELab IPS 3D Reconstructions of the Whole Heliosphere Interval and Comparison with in-Ecliptic Solar Wind Measurements from STEREO and Wind Instrumentation. , *256*(1-2), 201-217. doi: 10.1007/s11207-009-9350-9

Bisi, M. M., Jackson, B. V., Fallows, R. A., Dorrian, G. D., Manoharan, P. K., Clover, J. M., ... Tokumaru, M. (2010, May). Solar Wind and CME Studies of the Inner Heliosphere Using IPS Data from Stelab, ORT, and EISCAT. In *Advances in geosciences, volume 21: Solar terrestrial (st)* (Vol. 21, p. 33-49). doi: 10.1142/9789812838209_0003

Bisi, M. M., Thompson, B. J., Emery, B. A., Gibson, S. E., Leibacher, J., & van Driel-Gesztelyi, L. (2011, December). The Sun-Earth Connection near Solar Minimum: Placing it into Context. , *274*(1-2), 1-3. doi: 10.1007/s11207-011-9915-2

Blanc, M., Andrews, D. J., Coates, A. J., Hamilton, D. C., Jackman, C. M., Jia, X., … Westlake, J. H. (2015, October). Saturn Plasma Sources and Associated Transport Processes. , *192*(1-4), 237-283. doi: 10.1007/s11214-015-0172-9

Borovsky, J. E., & Denton, M. H. (2006, July). Differences between CME-driven storms and CIR-driven storms. *Journal of Geophysical Research (Space Physics)*, *111*(A7), A07S08. doi: 10.1029/2005JA011447

Bougher, S. W., Engel, S., Roble, R. G., & Foster, B. (2000, July). Comparative terrestrial planet thermospheres 3. Solar cycle variation of global structure and winds at solstices. , *105*(E7), 17669-17692. doi: 10.1029/1999JE001232

Bougher, S. W., Pawlowski, D., Bell, J. M., Nelli, S., McDunn, T., Murphy, J. R., … Ridley, A. (2015, February). Mars Global Ionosphere-Thermosphere Model: Solar cycle, seasonal, and diurnal variations of the Mars upper atmosphere. *Journal of Geophysical Research (Planets)*, *120*(2), 311-342. doi: 10.1002/2014JE004715

Breen, A. R., Mikic, Z., Linker, J. A., Lazarus, A. J., Thompson, B. J., Biesecker, D. A., … Lecinski, A. (1999). Interplanetary scintillation measurements of the solar wind during whole sun month: Comparisons with coronal and in situ observations. *Journal of Geophysical Research: Space Physics*, *104*(A5), 9847-9870. Retrieved from `https://agupubs.onlinelibrary.wiley.com/doi/abs/10.1029/1998JA900091` doi: https://doi.org/10.1029/1998JA900091

Breen, A. R., Thompson, B. J., Kojima, M., Biesecker, D. A., Canals, A., Fallows, R. A., … Williams, P. J. S. (2000, November). Measurements of the solar wind over a wide range of heliocentric distances - a comparison of results from the first three Whole Sun Months. *Journal of Atmospheric and Solar-Terrestrial Physics*, *62*(16), 1527-1543. doi: 10.1016/S1364-6826(00)00090-0

Bregou, E. J., Hudson, M. K., Kress, B. T., Qin, M., & Selesnick, R. S. (2022, July). Gleissberg Cycle Dependence of Inner Zone Proton Flux. *Space Weather*, *20*(7), e2022SW003072. doi: 10.1029/2022SW003072

Bromage, B. J. J., Alexander, D., Breen, A., Clegg, J. R., Del Zanna, G., DeForest, C., … Browning, P. K. (2000, April). Structure of a Large low-Latitude Coronal Hole. , *193*, 181-193. doi: 10.1023/A:1005209725885

Bruntz, R., Lopez, R. E., Bhattarai, S. K., Pham, K. H., Deng, Y., Huang, Y., … Lyon, J. G. (2012, July). Investigating the viscous interaction and its role in generating the ionospheric potential during the Whole Heliosphere Interval. *Journal of Atmospheric and Solar-Terrestrial Physics*, *83*, 70-78. doi: 10.1016/j.jastp.2012.03.016

Candido, C. M. N., Batista, I. S., Klausner, V., de Siqueira Negreti, P. M., Becker-Guedes, F., de Paula, E. R., … Correia, E. S. (2018, June). Response of the total electron content at Brazilian low latitudes to corotating interaction region and high-speed streams during solar minimum 2008. *Earth, Planets and Space*, *70*(1), 104. doi: 10.1186/s40623-018-0875-8

Chadney, J. M., Koskinen, T. T., Hu, X., Galand, M., Lavvas, P., Unruh, Y. C., … Yelle, R. V. (2022, January). Energy deposition in Saturn's equatorial upper atmosphere. , *372*, 114724. doi: 10.1016/j.icarus.2021.114724

Chamberlin, P. C., Woods, T. N., Crotser, D. A., Eparvier, F. G., Hock, R. A., & Woodraska, D. L. (2009, March). Solar cycle minimum measurements of the solar extreme ultraviolet spectral irradiance on 14 April 2008. , *36*(5), L05102. doi: 10.1029/2008GL037145

Clegg, J. R., Bromage, B. J. I., & Browning, P. K. (1999). Modeling the coronal magnetic field, with a new method for obtaining boundary conditions on the farside of the sun. *Journal of Geophysical Research: Space Physics*, *104* (A5), 9831-9846. Retrieved from https://agupubs.onlinelibrary.wiley.com/doi/abs/10.1029/1998JA900149 doi: https://doi.org/10.1029/1998JA900149

Cremades, H., Mandrini, C. H., & Dasso, S. (2011, December). Coronal Transient Events During Two Solar Minima: Their Solar Source Regions and Interplanetary Counterparts. , *274* (1-2), 233-249. doi: 10.1007/s11207-011-9769-7

de Toma, G. (2011, December). Evolution of Coronal Holes and Implications for High-Speed Solar Wind During the Minimum Between Cycles 23 and 24. , *274* (1-2), 195-217. doi: 10.1007/s11207-010-9677-2

Del Zanna, G., Gibson, S. E., Mason, H. E., Pike, C. D., & Mandrini, C. H. (2002, January). Sigmoidal diagnostics with SOHO/CDS. *Advances in Space Research*, *30* (3), 551-556. doi: 10.1016/S0273-1177(02)00341-1

Delamere, P. A., & Bagenal, F. (2010, October). Solar wind interaction with Jupiter's magnetosphere. *Journal of Geophysical Research (Space Physics)*, *115* (A10), A10201. doi: 10.1029/2010JA015347

Delamere, P. A., & Bagenal, F. (2013, November). Magnetotail structure of the giant magnetospheres: Implications of the viscous interaction with the solar wind. *Journal of Geophysical Research (Space Physics)*, *118* (11), 7045-7053. doi: 10.1002/2013JA019179

Delamere, P. A., Bagenal, F., Dols, V., & Ray, L. C. (2007, May). Saturn's neutral torus versus Jupiter's plasma torus. , *34* (9), L09105. doi: 10.1029/2007GL029437

Del Zanna, G., & Bromage, B. J. I. (1999). The elephant's trunk: Spectroscopic diagnostics applied to soho/cds observations of the august 1996 equatorial coronal hole. *Journal of Geophysical Research: Space Physics*, *104* (A5), 9753-9766. Retrieved from https://agupubs.onlinelibrary.wiley.com/doi/abs/10.1029/1998JA900067 doi: https://doi.org/10.1029/1998JA900067

Dobrzycka, D., Cranmer, S. R., Panasyuk, A. V., Strachan, L., & Kohl, J. L. (1999). Study of the latitudinal dependence of h i lyman and o vi emission in the solar corona: Evidence for the superradial geometry of the outflow in the polar coronal holes. *Journal of Geophysical Research: Space Physics*, *104* (A5), 9791-9799. Retrieved from https://agupubs.onlinelibrary.wiley.com/doi/abs/10.1029/1998JA900129 doi: https://doi.org/10.1029/1998JA900129

Dungey, J. W. (1961, January). Interplanetary Magnetic Field and the Auroral Zones. , *6* (2), 47-48. doi: 10.1103/PhysRevLett.6.47

Echer, E., Tsurutani, B. T., Gonzalez, W. D., & Kozyra, J. U. (2011, December). High Speed Stream Properties and Related Geomagnetic Activity During the Whole Heliosphere Interval (WHI): 20 March to 16 April 2008. , *274* (1-2), 303-320. doi: 10.1007/s11207-011-9739-0

Edberg, N. J. T., Nilsson, H., Futaana, Y., Stenberg, G., Lester, M., Cowley, S. W. H., … Zhang, T. L. (2011, September). Atmospheric erosion of Venus during stormy space weather. *Journal of Geophysical Research (Space Physics)*, *116* (A9), A09308. doi: 10.1029/2011JA016749

Eiscat, Ort, & Data, N. (2000, September). Observations of interplanetary scintillation during the 1998 Whole Sun Month: a comparison between. *Annales Geophysicae*, *18* (9), 1003-1008. doi: 10.5194/angeo-18-1003-2000

Emery, B. A., Richardson, I. G., Evans, D. S., Rich, F. J., & Wilson, G. R. (2011, December). Solar Rotational Periodicities and the Semiannual Variation in the Solar Wind, Radiation Belt, and Aurora. , *274* (1-2), 399-425. doi: 10.1007/s11207-011-9758-x

Emery, B. A., Richardson, I. G., Evans, D. S., Rich, F. J., & Xu, W. (2009). Solar wind structure sources and periodicities of global electron hemispheric power over three solar cycles. *Journal of Atmospheric and Solar-Terrestrial Physics*. doi: 10.1016/j.jastp.2008.08.005

Emmert, J. T., Lean, J. L., & Picone, J. M. (2010). Anomalously low solar extreme-ultraviolet irradiance and thermospheric density during solar minimum. *Geophys. Res. Lett.*, *37*.

Fang, X., Forbes, J. M., Benna, M., Montabone, L., Curry, S., & Jakosky, B. (2022, March). The Origins of Long-Term Variability in Martian Upper Atmospheric Densities. *Journal of Geophysical Research (Space Physics)*, *127*(3), e30145. doi: 10.1029/2021JA030145

Feynman, J., & Ruzmaikin, A. (2011, September). The Sun's Strange Behavior: Maunder Minimum or Gleissberg Cycle? , *272*(2), 351. doi: 10.1007/s11207-011-9828-0

Fludra, A., Del Zanna, G., Alexander, D., & Bromage, B. J. I. (1999). Electron density and temperature of the lower solar corona. *Journal of Geophysical Research: Space Physics*, *104*(A5), 9709-9720. Retrieved from `https://agupubs.onlinelibrary.wiley.com/doi/abs/10.1029/1998JA900033` doi: https://doi.org/10.1029/1998JA900033

Frazin, R. A., & Janzen, P. (2002, May). Tomography of the Solar Corona. II. Robust, Regularized, Positive Estimation of the Three-dimensional Electron Density Distribution from LASCO-C2 Polarized White-Light Images. , *570*(1), 408-422. doi: 10.1086/339572

Galvin, A. B., & Kohl, J. L. (1999). Whole sun month at solar minimum: An introduction. *Journal of Geophysical Research: Space Physics*, *104*(A5), 9673-9678. Retrieved from `https://agupubs.onlinelibrary.wiley.com/doi/abs/10.1029/1999JA900008` doi: https://doi.org/10.1029/1999JA900008

Gasperini, F., Hughes, J., & Thiemann, E. M. B. (2023, January). Solar Rotation Effects in Earth's and Mars' Thermospheric Densities as Revealed by Concurrent MAVEN, Swarm-C, and GOES Observations. *Journal of Geophysical Research (Planets)*, *128*(1), e2022JE007431. doi: 10.1029/2022JE007431

Gershman, D. J., & DiBraccio, G. A. (2020, December). Solar Cycle Dependence of Solar Wind Coupling With Giant Planet Magnetospheres. , *47*(24), e89315. doi: 10.1029/2020GL089315

Gibson, S. E. (2001, May). Global Solar Wind Structure from Solar Minimum to Solar Maximum: Sources and Evolution. , *97*, 69-79. doi: 10.1023/A:1011869926351

Gibson, S. E., Biesecker, D., Guhathakurta, M., Hoeksema, J. T., Lazarus, A. J., Linker, J., . . . Zhao, X. P. (1999, August). The Three-dimensional Coronal Magnetic Field during Whole Sun Month. , *520*(2), 871-879. doi: 10.1086/307496

Gibson, S. E., de Toma, G., Emery, B., Riley, P., Zhao, L., Elsworth, Y., . . . Webb, D. (2011, December). The Whole Heliosphere Interval in the Context of a Long and Structured Solar Minimum: An Overview from Sun to Earth. , *274*(1-2), 5-27. doi: 10.1007/s11207-011-9921-4

Gibson, S. E., Fletcher, L., Del Zanna, G., Pike, C. D., Mason, H. E., Mandrini, C. H., . . . Thompson, B. J. (2002, August). The Structure and Evolution of a Sigmoidal Active Region. , *574*(2), 1021-1038. doi: 10.1086/341090

Gibson, S. E., Fludra, A., Bagenal, F., Biesecker, D., Del Zanna, G., & Bromage, B. (1999). Solar minimum streamer densities and temperatures using whole sun month coordinated data sets. *Journal of Geophysical Research: Space Physics*, *104*(A5), 9691-9699. Retrieved from `https://agupubs.onlinelibrary.wiley.com/doi/abs/10.1029/98JA02681` doi: https://doi.org/10.1029/98JA02681

Gibson, S. E., Kozyra, J. U., de Toma, G., Emery, B. A., Onsager, T., & Thompson, B. J. (2009, September). If the Sun is so quiet, why is the Earth ringing? A comparison of two solar minimum intervals. *Journal of Geophysical Research (Space Physics)*, *114*(A9), A09105. doi: 10.1029/2009JA014342

Gibson, S. E., Kucera, T. A., Rastawicki, D., Dove, J., de Toma, G., Hao, J., . . . Zhang, M. (2010). Three-dimensional morphology of a coronal prominence

cavity. *Astrophys. J.*, *723*, 1133.
Gibson, S. E., Webb, D., Hewins, I. M., McFadden, R. H., Emery, B. A., Denig, W., & McIntosh, P. S. (2017). Beyond sunspots: Studies using the McIntosh Archive of global solar magnetic field patterns. In D. Nandy, A. Valio, & P. Petit (Eds.), *Living around active stars* (Vol. 328, p. 93). Cambridge University Press: Cambridge.
Gleissberg, W. (1944, January). a Table of Secular Variations of the Solar Cycle. *Terrestrial Magnetism and Atmospheric Electricity*, *49*(4), 243-244. doi: 10.1029/TE049i004p00243
Gopalswamy, N., Shibasaki, N., Thompson, B. J., Gurman, J., & DeForest, C. (1999). Microwave enhancement and variability in the elephant's trunk coronal hole: Comparison with soho observations. *Journal of Geophysical Research: Space Physics*, *104*(A5), 9767-9779. Retrieved from `https://agupubs.onlinelibrary.wiley.com/doi/abs/10.1029/1998JA900168` doi: https://doi.org/10.1029/1998JA900168
Guhathakurta, M., Fludra, A., Gibson, S. E., Biesecker, D., & Fisher, R. (1999). Physical properties of a coronal hole from a coronal diagnostic spectrometer, mauna loa coronagraph, and lasco observations during the whole sun month. *Journal of Geophysical Research: Space Physics*, *104*(A5), 9801-9808. Retrieved from `https://agupubs.onlinelibrary.wiley.com/doi/abs/10.1029/1998JA900082` doi: https://doi.org/10.1029/1998JA900082
Guhathakurta, M., Sittler, E. C., & Ofman, L. (2006, November). Semiempirically derived heating function of the corona heliosphere during the Whole Sun Month. *Journal of Geophysical Research (Space Physics)*, *111*(A11), A11215. doi: 10.1029/2006JA011931
Haberreiter, M. (2011, December). Solar EUV Spectrum Calculated for Quiet Sun Conditions. , *274*(1-2), 473-479. doi: 10.1007/s11207-011-9767-9
Hathaway, D. H. (2015, September). The Solar Cycle. *Living Reviews in Solar Physics*, *12*, 4. doi: 10.1007/lrsp-2015-4
Hewins, I. M., Gibson, S. E., & Emery, B. A. (2023 under review). WHPI Synoptic Coronal hole maps and solar wind studies. . (under review)
Hewins, I. M., Gibson, S. E., Webb, D. F., McFadden, R. H., A., K. T., & Emery, B. A. (2023 under review). Comparative Solar Minima using the McIntosh Archive. . (Paper under review, [Paper 2023JA031343])
Hewins, I. M., Gibson, S. E., Webb, D. F., McFadden, R. H., A., K. T., Emery, B. A., & McIntosh, S. W. (2020). The Evolution of Coronal Holes over Three Solar Cycles Using the McIntosh Archive. , *295*, 161. doi: 10.1007/s11207-020-01731-y
Hudson, M., Brito, T., Elkington, S., Kress, B., Li, Z., & Wiltberger, M. (2012, July). Radiation belt 2D and 3D simulations for CIR-driven storms during Carrington Rotation 2068. *Journal of Atmospheric and Solar-Terrestrial Physics*, *83*, 51-62. doi: 10.1016/j.jastp.2012.03.017
Hudson, M. K., Elkington, S. R., Li, Z., Patel, M., Pham, K., Sorathia, K., ... Leali, A. (2021, December). MHD-Test Particles Simulations of Moderate CME and CIR-Driven Geomagnetic Storms at Solar Minimum. *Space Weather*, *19*(12), e02882. doi: 10.1029/2021SW002882
Hughes, J., Gasperini, F., & Forbes, J. M. (2022, January). Solar Rotation Effects in Martian Thermospheric Density as Revealed by Five Years of MAVEN Observations. *Journal of Geophysical Research (Planets)*, *127*(1), e07036. doi: 10.1029/2021JE007036
Jackman, C. M., & Arridge, C. S. (2011, December). Solar Cycle Effects on the Dynamics of Jupiter's and Saturn's Magnetospheres. , *274*(1-2), 481-502. doi: 10.1007/s11207-011-9748-z
Jakosky, B. M., Grebowsky, J. M., Luhmann, J. G., Connerney, J., Eparvier, F., Ergun, R., ... Yelle, R. (2015, November). MAVEN observations of the response

of Mars to an interplanetary coronal mass ejection. *Science*, *350*(6261), 0210. doi: 10.1126/science.aad0210

Jian, L., Russell, C. T., Luhmann, J. G., & Skoug, R. M. (2006, December). Properties of Stream Interactions at One AU During 1995 2004. , *239*(1-2), 337-392. doi: 10.1007/s11207-006-0132-3

Ko, Y. K., Raymond, J. C., Gibson, S. E., Alexander, D., Strachan, L., Holzer, T., … Fletcher, L. (2005, April). Multialtitude Observations of a Coronal Jet during the Third Whole Sun Month Campaign. , *623*(1), 519-539. doi: 10.1086/428479

Lean, J. (1997, January). The Sun's Variable Radiation and Its Relevance For Earth. , *35*, 33-67. doi: 10.1146/annurev.astro.35.1.33

Lean, J. L., McDonald, S. E., Huba, J. D., Emmert, J. T., Drob, D. P., & Siefring, C. L. (2014, May). Geospace variability during the 2008-2009 Whole Heliosphere Intervals. *Journal of Geophysical Research (Space Physics)*, *119*(5), 3755-3776. doi: 10.1002/2013JA019485

Lee, C. O., Hara, T., Halekas, J. S., Thiemann, E., Chamberlin, P., Eparvier, F., … Jakosky, B. M. (2017, March). MAVEN observations of the solar cycle 24 space weather conditions at Mars. *Journal of Geophysical Research (Space Physics)*, *122*(3), 2768-2794. doi: 10.1002/2016JA023495

Lei, J., Thayer, J. P., Wang, W., & McPherron, R. L. (2011, December). Impact of CIR Storms on Thermosphere Density Variability during the Solar Minimum of 2008. , *274*(1-2), 427-437. doi: 10.1007/s11207-010-9563-y

Lepping, R. P., Wu, C. C., Berdichevsky, D. B., & Szabo, A. (2011, December). Magnetic Clouds at/near the 2007 - 2009 Solar Minimum: Frequency of Occurrence and Some Unusual Properties. , *274*(1-2), 345-360. doi: 10.1007/s11207-010-9646-9

Li, X., Schiller, Q., Blum, L., Califf, S., Zhao, H., Tu, W., … Spence, H. (2013, October). First results from CSSWE CubeSat: Characteristics of relativistic electrons in the near-Earth environment during the October 2012 magnetic storms. *Journal of Geophysical Research (Space Physics)*, *118*(10), 6489-6499. doi: 10.1002/2013JA019342

Li, Z., Hudson, M., & Chen, Y. (2014, March). Radial diffusion comparing a THEMIS statistical model with geosynchronous measurements as input. *Journal of Geophysical Research (Space Physics)*, *119*(3), 1863-1873. doi: 10.1002/2013JA019320

Lin, C.-H., & Chen, J. (2015, January). A Comparison of Coronal Mass Ejection Models with Observations for Two Large CMEs Detected During the Whole Heliosphere Interval. *Terrestrial, Atmospheric and Oceanic Sciences*, *26*(2-1), 121. doi: 10.3319/TAO.2014.10.15.01(AA)

Linker, J. A., Mikic, Z., Biesecker, D. A., Forsyth, R. J., E., G. S., Lazarus, A. J., … Thompson, B. J. (1999). Magnetohydrodynamic modeling of the solar corona during whole sun month. *Journal of Geophysical Research: Space Physics*, *104*(A5), 9809-9830. Retrieved from `https://agupubs.onlinelibrary.wiley.com/doi/abs/10.1029/1998JA900159` doi: https://doi.org/10.1029/1998JA900159

Lionello, R., Linker, J. A., & Mikić, Z. (2009, January). Multispectral Emission of the Sun During the First Whole Sun Month: Magnetohydrodynamic Simulations. , *690*(1), 902-912. doi: 10.1088/0004-637X/690/1/902

Lloveras, D. G., Vásquez, A. M., Nuevo, F. A., Frazin, R. A., Manchester, W., Sachdeva, N., … Gilardy, H. (2022, June). Three-Dimensional Structure of the Corona During WHPI Campaign Rotations CR-2219 and CR-2223. *Journal of Geophysical Research (Space Physics)*, *127*(6), e30406. doi: 10.1029/2022JA030406

Lopez, R. E., Bhattarai, S. K., Bruntz, R., Pham, K., Wiltberger, M., Lyon, J. G., … Huang, Y. (2012, July). The role of dayside merging in generating the ionospheric potential during the Whole Heliospheric Interval. *Journal of Atmospheric and Solar-Terrestrial Physics*, *83*, 63-69. doi: 10.1016/j.jastp.2012.03.001

Luhmann, J. G., Fedorov, A., Barabash, S., Carlsson, E., Futaana, Y., Zhang, T. L., ... Brain, D. A. (2008, August). Venus Express observations of atmospheric oxygen escape during the passage of several coronal mass ejections. *Journal of Geophysical Research (Planets)*, *113*(52), E00B04. doi: 10.1029/2008JE003092

Luhmann, J. G., Kasprzak, W. T., & Russell, C. T. (2007, April). Space weather at Venus and its potential consequences for atmosphere evolution. *Journal of Geophysical Research (Planets)*, *112*(E4), E04S10. doi: 10.1029/2006JE002820

Luhmann, J. G., Li, Y., Lee, C. O., Jian, L. K., Arge, C. N., & Riley, P. (2022, October). Solar Cycle Variability in Coronal Holes and Their Effects on Solar Wind Sources. *Space Weather*, *20*(10), e2022SW003110. doi: 10.1029/2022SW003110

Mauk, B. H., Fox, N. J., Kanekal, S. G., Kessel, R. L., Sibeck, D. G., & Ukhorskiy, A. (2013, November). Science Objectives and Rationale for the Radiation Belt Storm Probes Mission. , *179*(1-4), 3-27. doi: 10.1007/s11214-012-9908-y

McComas, D. J., & Bagenal, F. (2007, October). Jupiter: A fundamentally different magnetospheric interaction with the solar wind. , *34*(20), L20106. doi: 10.1029/2007GL031078

McComas, D. J., Bame, S. J., Barraclough, B. L., Feldman, W. C., Funsten, H. O., Gosling, J. T., ... Neugebauer, M. (1998). Ulysses' return to the slow solar wind. *Geophys. Res. Lett.*, *25*, 1-4. doi: 10.1029/97GL03444

McComas, D. J., Elliott, H. A., Schwadron, N. A., Gosling, J. T., Skoug, R. M., & Goldstein, B. E. (2003, May). The three-dimensional solar wind around solar maximum. *Geophys. Res. Lett.*, *30*, 1517. doi: 10.1029/2003GL017136

Mewaldt, R. A., Davis, A. J., L., K. A., L., A., R., Stone, E. C., ... von Rosenvinge, T. T. (2010). Record-setting cosmic-ray intensities in 2009 and 201. *Astrophys. J. Lett.*, *723*, 1.

Millan, R. M., & Thorne, R. M. (2007, March). Review of radiation belt relativistic electron losses. *Journal of Atmospheric and Solar-Terrestrial Physics*, *69*(3), 362-377. doi: 10.1016/j.jastp.2006.06.019

Mlynczak, M. G., Hunt, L. A., Garcia, R. R., Harvey, V. L., Marshall, B. T., Yue, J., ... Russell, J. M. (2022, November). Cooling and Contraction of the Mesosphere and Lower Thermosphere From 2002 to 2021. *Journal of Geophysical Research (Atmospheres)*, *127*(22), e2022JD036767. doi: 10.1029/2022JD036767

Moran, P. J., Ananthakrishnan, S., Balasubramanian, V., Breen, A. R., Canals, A., Fallows, R. A., ... Williams, P. J. S. (2000, September). Observations of interplanetary scintillation during the 1998 Whole Sun Month: a comparison between EISCAT, ORT and Nagoya data. *Annales Geophysicae*, *18*(9), 1003. doi: 10.1007/s00585-000-1003-0

Muller, R., Utz, D., & Hanslmeier, A. (2011, December). Non-Varying Granulation and Photospheric Network During the Extended 2007 - 2009 Solar Minimum. , *274*(1-2), 87-97. doi: 10.1007/s11207-011-9725-6

Nitta, N. V. (2011, December). Observables Indicating Two Major Coronal Mass Ejections During the WHI. , *274*(1-2), 219-232. doi: 10.1007/s11207-011-9806-6

Ogawa, Y., Seki, K., Keika, K., & Ebihara, Y. (2019, May). Characteristics of CME- and CIR-Driven Ion Upflows in the Polar Ionosphere. *Journal of Geophysical Research (Space Physics)*, *124*(5), 3637-3649. doi: 10.1029/2018JA025870

Palmerio, E., Lee, C. O., Richardson, I. G., Nieves-Chinchilla, T., Dos Santos, L. F. G., Gruesbeck, J. R., ... Luhmann, J. G. (2022, September). CME

Evolution in the Structured Heliosphere and Effects at Earth and Mars During Solar Minimum. *Space Weather*, *20*(9), e2022SW003215. doi: 10.1029/2022SW003215

Panasyuk, A. (1999). Three-dimensional reconstruction of uv emissivities in the solar corona using ultraviolet coronagraph spectrometer data from the whole sun month. *Journal of Geophysical Research: Space Physics*, *104*(A5), 9721-9726. Retrieved from `https://agupubs.onlinelibrary.wiley.com/doi/abs/10.1029/1998JA900118` doi: https://doi.org/10.1029/1998JA900118

Petrie, G. J. D., Canou, A., & Amari, T. (2011, December). Nonlinear Force-Free and Potential-Field Models of Active-Region and Global Coronal Fields during the Whole Heliosphere Interval. , *274*(1-2), 163-194. doi: 10.1007/s11207-010-9687-0

Pizzo, V. (1978, December). A three-deminsional model of corotating streams in the solar wind 1. Theoretical foundations. , *83*(A12), 5563-5572. doi: 10.1029/JA083iA12p05563

Poopakun, K., Nuntiyakul, W., Ruffolo, D., Evenson, P., Peng, J., Chuanraksasat, P., ... Oh, S. (2022, March). Solar magnetic polarity effect on neutron monitor count rates from latitude surveys versus Antarctic stations. In *37th international cosmic ray conference* (p. 1268). doi: 10.22323/1.395.01268

Posner, A., Bothmer, V., Thompson, B. J., Kunow, H., Heber, B., Mueller-Mellin, R., ... Linker, J. A. (1999). In-ecliptic cir-associated energetic particle events and polar coronal hole structures: Soho/costep observations for the whole sun month campaign. *Journal of Geophysical Research: Space Physics*, *104*(A5), 9881-9890. Retrieved from `https://agupubs.onlinelibrary.wiley.com/doi/abs/10.1029/98JA02654` doi: https://doi.org/10.1029/98JA02654

Potgieter, M. S. (2013, June). Solar Modulation of Cosmic Rays. *Living Reviews in Solar Physics*, *10*(1), 3. doi: 10.12942/lrsp-2013-3

Riley, P., Caplan, R. M., Downs, C., Linker, J. A., & Lionello, R. (2022, August). Comparing and Contrasting the Properties of the Inner Heliosphere for the Three Most Recent Solar Minima. *Journal of Geophysical Research (Space Physics)*, *127*(8), e30261. doi: 10.1029/2022JA030261

Riley, P., Downs, C., Linker, J. A., Mikic, Z., Lionello, R., & Caplan, R. M. (2019, April). Predicting the Structure of the Solar Corona and Inner Heliosphere during Parker Solar Probe's First Perihelion Pass. , *874*(2), L15. doi: 10.3847/2041-8213/ab0ec3

Riley, P., Gosling, J. T., McComas, D. J., Pizzo, V. J., Luhmann, J. G., Biesecker, D., ... Thompson, B. J. (1999). Relationship between ulysses plasma observations and solar observations during the whole sun month campaign. *Journal of Geophysical Research: Space Physics*, *104*(A5), 9871-9879. Retrieved from `https://agupubs.onlinelibrary.wiley.com/doi/abs/10.1029/1998JA900078` doi: https://doi.org/10.1029/1998JA900078

Riley, P., Linker, J. A., & Mikić, Z. (2001, August). An empirically-driven global MHD model of the solar corona and inner heliosphere. , *106*(A8), 15889-15902. doi: 10.1029/2000JA000121

Riley, P., Lionello, R., Linker, J. A., Mikic, Z., Luhmann, J., & Wijaya, J. (2011, December). Global MHD Modeling of the Solar Corona and Inner Heliosphere for the Whole Heliosphere Interval. , *274*(1-2), 361-377. doi: 10.1007/s11207-010-9698-x

Schwadron, N. A., Rahmanifard, F., Wilson, J., Jordan, A. P., Spence, H. E., Joyce, C. J., ... Zeitlin, C. (2018, March). Update on the Worsening Particle Radiation Environment Observed by CRaTER and Implications for Future Human Deep-Space Exploration. *Space Weather*, *16*(3), 289-303. doi: 10.1002/2017SW001803

Slavin, J. A., Middleton, H. R., Raines, J. M., Jia, X., Zhong, J., Sun, W. J., ... Mays, M. L. (2019, August). MESSENGER Observations of Disappearing

Dayside Magnetosphere Events at Mercury. *Journal of Geophysical Research (Space Physics)*, *124*(8), 6613-6635. doi: 10.1029/2019JA026892

Solomon, S. C., Burns, A. G., Emery, B. A., Mlynczak, M. G., Qian, L., Wang, W., ... Wiltberger, M. (2012, August). Modeling studies of the impact of high-speed streams and co-rotating interaction regions on the thermosphere-ionosphere. *Journal of Geophysical Research (Space Physics)*, *117*, A00L11. doi: 10.1029/2011JA017417

Solomon, S. C., Qian, L., Didkovsky, L. V., Viereck, R. A., & Woods, T. N. (2011). Causes of low thermospheric density during the 2007 - 2009 solar minimum. *J. Geophys. Res.*, *116*. doi: 10.1029/2011JA016508

Strachan, L., Ko, Y. K., Panasyuk, A. V., Dobrzycka, D., Kohl, J. L., Romoli, M., ... Biesecker, D. A. (1999, January). Constraints on Coronal Outflow Velocities Derived from UVCS Doppler Dimming Measurements and in-Situ Charge State Data. , *87*, 311-314. doi: 10.1023/A:1005193711445

Strachan, L., Panasyuk, A. V., Dobrzycka, D., Kohl, J. L., Noci, G., Gibson, S. E., & Biesecker, D. A. (2000, February). Latitudinal dependence of outflow velocities from O VI Doppler dimming observations during the Whole Sun Month. , *105*(A2), 2345-2356. doi: 10.1029/1999JA900459

Temmer, M. (2021, December). Space weather: the solar perspective. *Living Reviews in Solar Physics*, *18*(1), 4. doi: 10.1007/s41116-021-00030-3

Thiemann, E. M. B., Eparvier, F. G., Bougher, S. W., Dominique, M., Andersson, L., Girazian, Z., ... Jakosky, B. M. (2018, September). Mars Thermospheric Variability Revealed by MAVEN EUVM Solar Occultations: Structure at Aphelion and Perihelion and Response to EUV Forcing. *Journal of Geophysical Research (Planets)*, *123*(9), 2248-2269. doi: 10.1029/2018JE005550

Thompson, B. J., Gibson, S. E., Schroeder, P. C., Webb, D. F., Arge, C. N., Bisi, M. M., ... Woods, T. N. (2011, December). A Snapshot of the Sun Near Solar Minimum: The Whole Heliosphere Interval. , *274*(1-2), 29-56. doi: 10.1007/s11207-011-9891-6

Torsti, J., Anttila, A., & Sahla, T. (1999). Concurrent solar and corotating interaction region particle events in august 1996. *Journal of Geophysical Research: Space Physics*, *104*(A5), 9891-9902. Retrieved from `https://agupubs.onlinelibrary.wiley.com/doi/abs/10.1029/1998JA900170` doi: https://doi.org/10.1029/1998JA900170

Torsti, J., Kocharov, L., Teittinen, M., Anttila, A., Laitinen, T., Makela, P., ... Valtonen, E. (1999). Energetic (10–65 mev) protons observed by erne on august 13–14, 1996: Eruption on the solar back side as a possible source of the event. *Journal of Geophysical Research: Space Physics*, *104*(A5), 9903-9909. Retrieved from `https://agupubs.onlinelibrary.wiley.com/doi/abs/10.1029/1998JA900017` doi: https://doi.org/10.1029/1998JA900017

Tsurutani, B. T., Gonzalez, W. D., Gonzalez, A. L. C., Guarnieri, F. L., Gopalswamy, N., Grande, M., ... Vasyliunas, V. (2006, July). Corotating solar wind streams and recurrent geomagnetic activity: A review. *Journal of Geophysical Research (Space Physics)*, *111*(A7), A07S01. doi: 10.1029/2005JA011273

Varela, J., Brun, A. S., Zarka, P., Strugarek, A., Pantellini, F., & Réville, V. (2022, November). MHD Study of Extreme Space Weather Conditions for Exoplanets With Earth-Like Magnetospheres: On Habitability Conditions and Radio-Emission. *Space Weather*, *20*(11), e2022SW003164. doi: 10.1029/2022SW003164

Vásquez, A. M., Huang, Z., Manchester, W. B., & Frazin, R. A. (2011, December). The WHI Corona from Differential Emission Measure Tomography. , *274*(1-2), 259-284. doi: 10.1007/s11207-010-9706-1

Vasyliunas, V. M. (1983). Physics of the Jovian magnetosphere. 11. Plasma distribution and flow. In *Physics of the jovian magnetosphere* (p. 395-453).

Vasyliunas, V. M. (1986, July). The convection-dominated magnetosphere of

Uranus. , *13*(7), 621-623. doi: 10.1029/GL013i007p00621
Verkhoglyadova, O. P., Tsurutani, B. T., Mannucci, A. J., Mlynczak, M. G., Hunt, L. A., Komjathy, A., & Runge, T. (2011, September). Ionospheric VTEC and thermospheric infrared emission dynamics during corotating interaction region and high-speed stream intervals at solar minimum: 25 March to 26 April 2008. *Journal of Geophysical Research (Space Physics)*, *116*(A9), A09325. doi: 10.1029/2011JA016604
Wang, W., Lei, J., Burns, A. G., Qian, L., Solomon, S. C., Wiltberger, M., & Xu, J. (2011, December). Ionospheric Day-to-Day Variability Around the Whole Heliosphere Interval in 2008. , *274*(1-2), 457-472. doi: 10.1007/s11207-011-9747-0
Wang, Y.-M., & Sheeley, N. R. J. (1990). Solar wind speed and coronal flux-tube expansion. *Astrophys. J.*, *355*, 726.
Wang, Y.-M., & Sheeley, N. R. J. (1991). Why fast solar wind originates from slowly expanding coronal flux tubes. *Astrophys. J. Lett.*, *372*, 45.
Warren, H. P., & Hassler, D. M. (1999). The density structure of a solar polar coronal hole. *Journal of Geophysical Research: Space Physics*, *104*(A5), 9781-9789. Retrieved from `https://agupubs.onlinelibrary.wiley.com/doi/abs/10.1029/1998JA900079` doi: https://doi.org/10.1029/1998JA900079
Webb, D. F., Cremades, H., Sterling, A. C., Mandrini, C. H., Dasso, S., Gibson, S. E., … Plunkett, S. P. (2011, December). The Global Context of Solar Activity During the Whole Heliosphere Interval Campaign. , *274*(1-2), 57-86. doi: 10.1007/s11207-011-9787-5
Webb, D. F., Gibson, S. E., Hewins, I. M., McFadden, R. H., Emery, B. A., Malanushenko, A., & Kuchar, T. (2018). Global solar magnetic field evolution over 4 solar cycles: Use of the mcintosh archive. *Frontiers in Astronomy and Space Sciences*.
Welsch, B. T., Christe, S., & McTiernan, J. M. (2011, December). Photospheric Magnetic Evolution in the WHI Active Regions. , *274*(1-2), 131-157. doi: 10.1007/s11207-011-9759-9
White, O., Kopp, G., Snow, M., & Tapping, K. (2011, December). The Solar Cycle 23 - 24 Minimum. A Benchmark in Solar Variability and Effects in the Heliosphere. , *274*(1-2), 159-162. doi: 10.1007/s11207-010-9680-7
Wijsen, N., Samara, E., Aran, À., Lario, D., Pomoell, J., & Poedts, S. (2021, February). A Self-consistent Simulation of Proton Acceleration and Transport Near a High-speed Solar Wind Stream. , *908*(2), L26. doi: 10.3847/2041-8213/abe1cb
Wiltberger, M., Qian, L., Huang, C.-L., Wang, W., Lopez, R. E., Burns, A. G., … Huang, Y. (2012, July). CMIT study of CR2060 and 2068 comparing L1 and MAS solar wind drivers. *Journal of Atmospheric and Solar-Terrestrial Physics*, *83*, 39-50. doi: 10.1016/j.jastp.2012.01.005
Wiltberger, M., Rigler, E. J., Merkin, V., & Lyon, J. G. (2017, March). Structure of High Latitude Currents in Magnetosphere-Ionosphere Models. , *206*(1-4), 575-598. doi: 10.1007/s11214-016-0271-2
Winslow, R. M., Lugaz, N., Philpott, L., Farrugia, C. J., Johnson, C. L., Anderson, B. J., … Asad, M. A. (2020, February). Observations of Extreme ICME Ram Pressure Compressing Mercury's Dayside Magnetosphere to the Surface. , *889*(2), 184. doi: 10.3847/1538-4357/ab6170
Witasse, O., Sánchez-Cano, B., Mays, M. L., Kajdič, P., Opgenoorth, H., Elliott, H. A., … Altobelli, N. (2017, August). Interplanetary coronal mass ejection observed at STEREO-A, Mars, comet 67P/Churyumov-Gerasimenko, Saturn, and New Horizons en route to Pluto: Comparison of its Forbush decreases at 1.4, 3.1, and 9.9 AU. *Journal of Geophysical Research (Space Physics)*, *122*(8), 7865-7890. doi: 10.1002/2017JA023884
Woods, T. N., Chamberlin, P. C., Harder, J. W., Hock, R. A., Snow, M., Eparvier,

F. G., . . . Richard, E. C. (2009, January). Solar Irradiance Reference Spectra (SIRS) for the 2008 Whole Heliosphere Interval (WHI). , *36*(1), L01101. doi: 10.1029/2008GL036373

Woods, T. N., Harder, J. W., Kopp, G., & Snow, M. (2022, April). Solar-Cycle Variability Results from the Solar Radiation and Climate Experiment (SORCE) Mission. , *297*(4), 43. doi: 10.1007/s11207-022-01980-z

Younas, W., Khan, M., Amory-Mazaudier, C., & Amaechi, P. O. (2022, December). Ionospheric Response to the Coronal Hole Activity of August 2020: A Global Multi-Instrumental Overview. *Space Weather*, *20*(12), e2022SW003176. doi: 10.1029/2022SW003176

Zhao, L., & Fisk, L. (2011, December). Understanding the Behavior of the Heliospheric Magnetic Field and the Solar Wind During the Unusual Solar Minimum Between Cycles 23 and 24. , *274*(1-2), 379-397. doi: 10.1007/s11207-011-9840-4

Zhao, X. P., Hoeksema, J. T., & Scherrer, P. H. (1999). Changes of the boot-shaped coronal hole boundary during whole sun month near sunspot minimum. *Journal of Geophysical Research: Space Physics*, *104*(A5), 9735-9751. Retrieved from `https://agupubs.onlinelibrary.wiley.com/doi/abs/10.1029/1998JA900010` doi: https://doi.org/10.1029/1998JA900010

Zidowitz, S. (1999). Coronal structure of the whole sun month: A tomographic reconstruction. *Journal of Geophysical Research: Space Physics*, *104*(A5), 9727-9734. Retrieved from `https://agupubs.onlinelibrary.wiley.com/doi/abs/10.1029/1998JA900099` doi: https://doi.org/10.1029/1998JA900099

Whole Heliosphere and Planetary Interactions (WHPI): The Big Picture on Solar Cycle Minima

Sarah E. Gibson[1], Robert C. Allen[2], Giuliana de Toma[1], Barbara Emery[1], Federico Gasperini[3], Ian Hewins[1,3], Mary Hudson[1], Liying Qian[1], and Barbara Thompson[4]

[1]High Altitude Observatory, National Center for Atmospheric Research, Boulder, CO 80305, USA
[2]Johns Hopkins University Applied Physics Laboratory, Laurel, MD, 20723, USA
[3]Orion Space Solutions, Louisville, CO 80027, USA
[4]NASA, Goddard Space Flight Center, Heliophysics Science Division, Greenbelt, MD 20771, USA

Key Points:

- The Whole Heliosphere and Planetary Interactions initiative studies the solar-heliospheric-planetary system's response to solar minimum.
- Solar minimum time periods provide an opportunity to characterize the baseline system and to trace events from "end to end".
- By comparing solar minima of multiple solar cycles, we gain insight into how the system changes over decadal times scales.

Corresponding author: Sarah Gibson, `sgibson@ucar.edu`

Abstract

The Whole Heliosphere and Planetary Interactions (WHPI) is an international initiative to study the most recent solar minimum and its impact on the interconnected solar-heliospheric-planetary system by facilitating and encouraging interdisciplinary activities. Particular WHPI science foci include the global connected structure of the heliosphere and planetary space environments/atmospheres, the origins and impacts of high-speed solar wind streams, coronal mass ejections (CMEs) from Sun-to-Heliopause, and comparative solar minima. This is achieved through a series of coordinated observing campaigns, including Parker Solar Probe perihelia, and scientific virtual interactions including a dedicated workshop where observers and modelers gathered to discuss, compare, and combine research results. This introduction sets the scene for the WHPI interval, placing it into the context of prior initiatives and describing the overall evolution of the system between 2018-2020. Along with the accompanying articles, it presents a selection of key scientific results on the interconnected solar-heliospheric-planetary system at solar minimum.

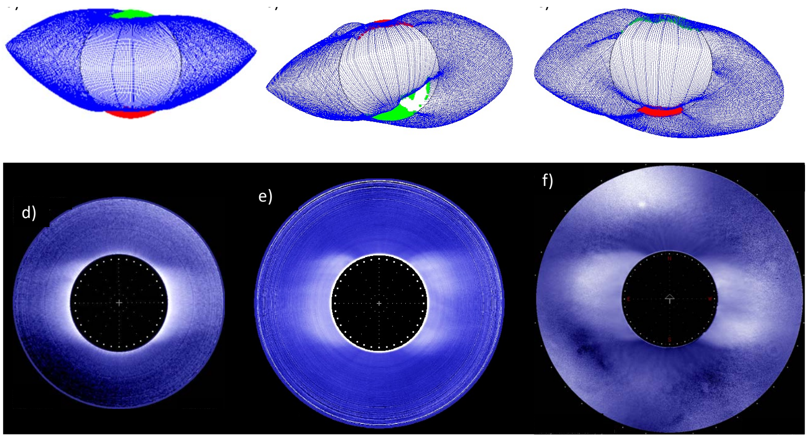

Figure 1. Three solar minima: 1996 Whole Sun Month (WSM); 2008-2009 Whole Heliosphere Interval (WHI); 2019-2020 Whole Heliosphere and Planetary Interactions (WHPI). a-c) National Solar Observatory Global Oscillations Network Group (NSO-GONG) line-of-sight coronal hole plots obtained from a potential field source surface extrapolation from solar surface magnetic fields (`https://gong.nso.edu/data/magmap/QR/bqg/`) for (left to right) January 31, 1996 (about six months before the official WSM solar rotation, and representative of that solar minimum's strongly dipolar structure); December 4, 2008 (WHI2 (Gibson et al., 2009); a rotation of relatively simple coronal structure); March 22, 2019 (Approximately midway through WHPI; a time of relatively simple coronal structure (see Section 4)). d-f) Mauna Loa Solar Observatory (MLSO) white light coronagraph images for the same three dates `https://mlso.hao.ucar.edu/mlso_data_calendar.php`).

1 Introduction

Why study solar minimum? Isn't it boring? After all, solar activity waxes and wanes with sunspot number, and, at solar minimum, it is definitely wane time (Hathaway, 2015). Solar flares and coronal mass ejections (CMEs) and their associated space-weather impacts at the Earth and other planets reach their lowest ebb during solar sunspot minimum (Temmer, 2021). However, as this paper and referenced articles demonstrate, there is more to the Sun and its impact on the heliosphere and planets than the activity associated with sunspots. In addition, when things are simple, end-to-end connections are easier to trace. Finally, solar minimum presents an opportunity to characterize the baseline, or ground state, of the heliosphere and planetary environments, and to consider how this baseline changes from one solar cycle to the next.

The Whole Heliosphere and Planetary Interactions (WHPI) is an international initiative focused on the solar minimum period. WHPI follows two similar initiatives during previous solar minima. Each initiative has expanded in scope, from Sun-to-solar-wind science during the Whole Sun Month (WSM) of 1996, to Sun-to-solar-wind-to-geospace science during the Whole Heliosphere Intervals (WHI) of 2008-2009, to the studies of Sun-to-solar-wind-to-planetary interactions of WHPI in 2018-2020 (Figure 1). The success of these efforts relies on a broad participation of scientists worldwide and across disciplines, and with each iteration such participation has increased. The WHPI mailing list currently has 777 subscriptors and continues to grow, and the September 2021 WHPI workshop had over 200 registered participants from 30 countries, resulting in a broad variety of talks and posters and a vibrant community discussion that has informed and enriched this introductory paper.

The structure of this paper is as follows. Section 2 describes the interconnected system at solar minimum, from Sun to solar wind, and from Sun to solar wind to planets. Section 3 provides a brief history of the "whole" intervals, for which WHPI is the third data point, and discusses WHPI in the context of these and other solar minima. Section 4 steps through "a year in the life" of the WHPI solar minimum, demonstrating the fascinating science that these quiet time periods inspire. Finally, Section 5 presents our conclusions.

2 The Interconnected System at Solar Minimum

2.1 From Sun to Solar Wind

The heliosphere is filled with a solar wind that originates from and is structured by the Sun's magnetic fields. Most of our observations of the solar wind are obtained *in situ*, by sending a satellite into space and measuring solar wind properties locally. A significant boost to our understanding came when the Ulysses satellite (McComas et al., 1998, 2003) moved out of the ecliptic, firmly establishing that fast wind emerges from the dark coronal holes seen in solar observations (Figure 2b). At solar minimum, this fast wind is primarily from the well-established polar coronal holes (Figure 2a), and slow wind is centered on the equator where bright coronal streamers trace out the predominantly dipolar magnetic structure of the Sun's corona (Figure 1).

This is somewhat of an over-simplification: we will discuss the importance of low-latitude high-speed solar wind streams at solar minimum and during the declining phase leading up to solar minimum, and, as we will see in Section 3, some solar minima have more magnetic complexity than others. Nevertheless, it is certainly true that solar minima are less complex than solar maxima, which are characterized by mixed fast and slow solar-wind speed at all latitudes. Solar maxima are also more dynamic than solar minima, with multiple coronal mass ejections expanding out through the heliosphere on any given day. Interestingly, the increase of structure and dynamics in the heliosphere at maximum results in a suppression of galactic cosmic rays (GCRs) so that when sunspot number is high at the Sun, GCR levels in the heliosphere are low, while at solar minimum, GCR levels reach their maximum level (Potgieter, 2013; Poopakun et al., 2022).

The source regions of high-speed solar wind observed at the Earth are generally low-latitude (near-equatorial) coronal holes – which can occur even during solar mini-

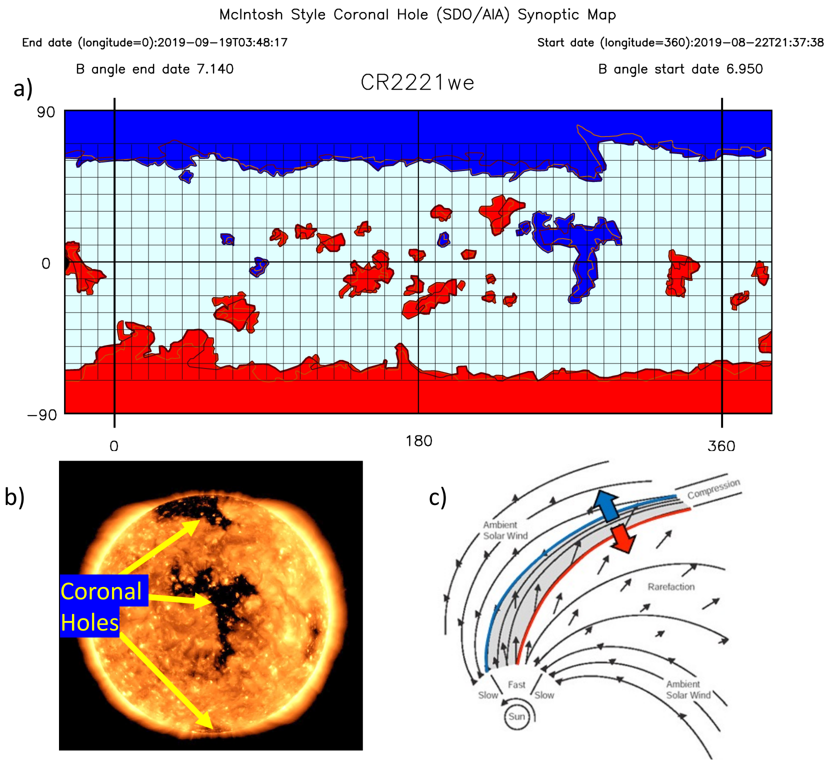

Figure 2. Fast solar wind originates in magnetically-open coronal holes. a) Example of a solar synoptic (latitude vs longitude) McIntosh Archive style map (Gibson et al., 2017; Webb et al., 2018, `https://www2.hao.ucar.edu/mcintosh-archive`) developed for WHPI (Hewins, Gibson, Webb, et al., 2023 under review, for this collection). The map is from Carrington Rotation 2221, August 22 - September 19, 2019. Coronal holes are represented in blue (positive magnetic polarity) and red (negative magnetic polarity). The polar coronal holes extend across all longitudes at both poles, but lower latitude (equatorial) coronal holes also exist. The large T-shaped blue (positive polarity) coronal hole centered around 270° solar longitude is discussed in further detail in Section 4.3, and seen in b) EUV image (SDO/AIA; March 29, 2019). c) Schematic diagram (view from heliographic pole) of fast wind catching up with slow wind and creating a Stream Interaction Region (SIR; adapted from Pizzo (1978) and Jian et al. (2006)).

mum (Figure 2b). Global magnetic models that use observations of the magnetic field at the Sun's surface, or photosphere, as a boundary condition (e.g., Figure 1a-c) find that when magnetic field lines extending out from the core of coronal holes line up with a spacecraft that samples the solar wind *in situ*, they are the source of high-speed solar wind streams (Wang & Sheeley, 1990, 1991; Riley et al., 2019). As the Sun rotates, solar wind emerges in a spiral pattern (Figure 2c), and if fast wind from a low-latitude coronal hole catches up with slower wind in front of it, it can create a Stream Interaction Regions (SIR; (Pizzo, 1978)) of compressed magnetized plasma that can drive space weather. If the low-latitude coronal hole lives for multiple solar rotations, these become Corotating Interaction Regions (CIRs) and act as periodic drivers of the solar wind and planetary environments. Since most of the interaction regions described in this paper persist, the terms SIR, CIR, and high-speed solar wind stream will essentially be used interchangeably for the remainder of the paper.

2.2 From Sun to Solar Wind to Planets

Because of the prevalence of long-lived low-latitude coronal holes during the months leading up to solar minima (Hewins et al., 2020), SIRs are the dominant drivers of space weather at the Earth and other planets during low-solar-activity times (Tsurutani et al., 2006). Although they do not have the coherent, rotating magnetic structure of CMEs, SIRs are otherwise quite similar in that they are characterized by a jump in dynamic pressure along with increased velocity and magnetic field strength (Bingham et al., 2018). As a consequence, SIRs compress planetary bowshocks and magnetopauses (Borovsky & Denton, 2006).

In general, the sensitivity of planetary magnetospheres to such solar wind forcing varies from planet to planet (Bagenal, 2013) (and from star to star; see Varela et al. (2022)). In the solar system, Jupiter and Saturn's magnetic fields are much stronger than Earth's, and their magnetospheres are only weakly driven by the solar wind as they are dominated by internal forcing (Vasyliunas, 1983; McComas & Bagenal, 2007; Delamere & Bagenal, 2010, 2013) with primary sources of plasma to their magnetospheres coming from their satellites, Io and Enceladus (Delamere et al., 2007; Blanc et al., 2015; Allen et al., 2018; Bagenal & Dols, 2020). The nature of Uranus and Neptune's magnetospheres are less well-understood, but Gershman and DiBraccio (2020) argued that, due to their highly tilted rotation relative to their magnetic dipoles, solar-wind driving may play an important role in convection within their magnetospheres (Vasyliunas, 1986). In contrast, there is no question about the Earth's magnetospheric response to external processes, as reconnection in the magnetotail drives auroral precipitation at the poles and plasma convection at Earth's high latitudes (Dungey, 1961). Mercury is also dominated by external forcing, not surprisingly due to its extreme proximity to the Sun. For the most extreme CME events, its dayside magnetosphere disappears, leaving Mercury exposed to the solar wind (Slavin et al., 2019; Winslow et al., 2020). This is always true at Mars, which has an induced magnetosphere and is only weakly shielded from impacts by solar and interplanetary disturbances (Jakosky et al., 2015; Lee et al., 2017). Venus also has an induced magnetosphere and auroral processes that depend upon solar wind pressure (Luhmann et al., 2007, 2008; Edberg et al., 2011).

The effects of solar wind forcing on a planetary magnetosphere and atmosphere has been most comprehensively observed at the Earth, where both CMEs and SIRs drive geomagnetic storms (Borovsky & Denton, 2006). These in turn lead to enhanced wave activity, auroral and radiation belt particle precipitation (Bingham et al., 2018; Millan & Thorne, 2007), which leads to an increase in ionospheric temperature, plasma density, and ion upflows and outflows (Wang et al., 2011; Ogawa et al., 2019) and also impacts Earth's neutral atmosphere (thermosphere) thermal structure, density and composition (Solomon et al., 2012; Younas et al., 2022, a paper in this collection). When there is a CIR surviving for multiple rotations, the result is periodic forcing of the Earth's space environment and upper atmosphere. Such periodicities are observed in a range of indices including geomagnetic indices, total electron content (ionosphere), neutral density (thermosphere), and energetic electrons (radiation belt) (Gibson et al., 2010; Emery et al., 2009; Lei et al., 2011). We will return to this in Section 4.

As we will also discuss further in Section 4, SIRs in the solar wind have been observed by the Mars Atmosphere and Volatile EvolutioN (MAVEN) satellite in orbit around Mars. In the Martian atmosphere, it can be difficult to separate out the effects of periodic particulate (solar wind) forcing vs radiative forcing. The most common periodic radiative forcing comes from the Sun's 27-day rotation which arises from any large long-lived solar active region (or indeed any long-lived solar feature) (J. Lean, 1997). Hughes et al. (2022) compared MAVEN solar irradiance observations with measurements of Mars thermospheric densities, and found clear correlations, especially at high altitudes. In a related study, Gasperini et al. (2023, a paper in this collection) compared the response of Mars' and Earth's thermospheres to EUV variation at solar minimum vs solar maximum and found greatly increased response of the middle thermospheric densities to solar rotation during the time of reduced EUV forcing at solar minimum for both planets. This may be explained by a reduction in adiabatic cooling due to rising motions in global circulation at low and middle terrestrial latitudes during solar minimum (Bougher et al., 2000, 2015).

Further subtleties arise at Mars because different wavelengths of light drive different reactions at different heights in the atmosphere (Thiemann et al., 2018). In particular, EUV wavelengths drive a direct effect involving local heating that has greatest impact in the upper Martian atmosphere, while infrared (IR) irradiance, which varies with variations in Mars' orbital distance from the Sun, has an indirect effect through upward coupling from the cooled lower-middle atmosphere. As a result, for high altitudes in the Mars atmosphere at solar maximum, the EUV effect may dominate compared to the solar-cycle-independent orbital (IR) effect, while at solar minimum, the EUV effect plays a relatively minor role (Fang et al., 2022).

3 Comparative Solar Minima

3.1 A Brief History of the "Whole Intervals"

The first of the "Whole" minimum campaigns was the Whole Sun Month (WSM) which occurred during a "classic" solar minimum in 1996. The solar corona was characterized by a global dipole field with streamer belts at the equator and large coronal holes at both poles (Figure 1a,d) as well as one equatorial coronal hole extension known as the Elephant's Trunk, which was the source of a fast wind stream impacting the Earth. The papers coming out of WSM marked the opening of the floodgates of Sun/solar wind scientific collaborations inspired by the SOHO satellite (Torsti, Anttila, & Sahla, 1999; Fludra et al., 1999; Linker et al., 1999; Del Zanna & Bromage, 1999; Dobrzycka et al., 1999; Biesecker et al., 1999; Warren & Hassler, 1999; Riley et al., 1999; Guhathakurta et al., 1999; Clegg et al., 1999; Breen et al., 1999; Panasyuk, 1999; Galvin & Kohl, 1999; Posner et al., 1999; Alexander, 1999; Gopalswamy et al., 1999; Torsti, Kocharov, et al., 1999; Zidowitz, 1999; Zhao et al., 1999; Gibson et al., 1999; Strachan et al., 1999; Gibson et al., 1999; Strachan et al., 2000; Bromage et al., 2000; Riley et al., 2001; Frazin & Janzen, 2002; Guhathakurta et al., 2006; Lionello et al., 2009).

This first WSM initiative focused on just one solar rotation (August 10-September 8, 1996) during solar minimum, but was followed by two related campaigns in 1998 (WSM2) and 1999 (WSM3) (Eiscat et al., 2000; Moran et al., 2000; Breen et al., 2000; Gibson et al., 2002; Gibson, 2001; Del Zanna et al., 2002; Ko et al., 2005).

The next solar minimum saw the organization of the Whole Heliosphere Interval (WHI) in 2008. The scope was expanded from Sun to Earth, and dozens of solar, heliospheric, and geospace instruments were involved. The WHI minimum was surprisingly different than WSM and other prior space-age solar minima. Despite an extremely low number of sunspots, there was more structure in the corona and heliosphere, with multiple broad low-latitude coronal holes and periodic forcing of the earth's space environment by high speed streams in 2008 (WHI1: CR2068, March 20 - April 16, 2008). The WHI minimum continued to evolve and become even quieter in 2009, becoming longer and deeper than any space-age solar minimum witnessed prior to it (WHI2/WHI3: CR2078/ CR2085, December 17, 2008 - January 12, 2009/ June 26 – July 22, 2009). The high-speed streams faded out, resulting in extreme depletion of radiation belt electrons at Earth (X. Li et al., 2013), as well as weak interplanetary magnetic field and record high levels of galactic cosmic rays (Mewaldt et al., 2010; Schwadron et al., 2018). However, the Sun's corona never became as predominantly dipolar as in 1996 (Figure 1), possibly because the polar magnetic fields in 2009 were significantly weaker than in 1996.

WHI science was rich, with analyses continuing for years after the original campaign time periods (Woods et al., 2009; Chamberlin et al., 2009; Bisi et al., 2009; Gibson et al., 2009; Bisi et al., 2010; Verkhoglyadova et al., 2011; Bisi et al., 2011; Gibson et al., 2011; Thompson et al., 2011; Webb et al., 2011; Muller et al., 2011; Welsch et al., 2011; White et al., 2011; Petrie et al., 2011; de Toma, 2011; Nitta, 2011; Cremades et al., 2011; Altrock, 2011; Vásquez et al., 2011; Benito et al., 2022; Echer et al., 2011; Lepping et al., 2011; Riley et al., 2011; Zhao & Fisk, 2011; Emery et al., 2011; Lei et al., 2011; Araujo-Pradere et al., 2011; Wang et al., 2011, 2011; Haberreiter, 2011; Jackman & Arridge, 2011; Wiltberger et al., 2012; Hudson et al., 2012; Lopez et al., 2012; Bruntz et al., 2012; Solomon et al., 2012; Z. Li et al., 2014; J. L. Lean et al., 2014; Lin & Chen, 2015; Wiltberger et al., 2017; Candido et al., 2018; Chadney et al., 2022).

The third iteration was the Whole Heliosphere and Planetary Interactions (WHPI). Based on lessons learned from WSM and WHI, the interval was not confined to a few solar rotations, but covered the period from late 2018 through early 2020. The level of participation increased with its expanded scope encompassing Sun to solar wind to planetary magnetospheres and atmospheres. The articles accompanying this introduction (Hudson et al., 2021; Lloveras et al., 2022; Riley et al., 2022; Gasperini et al., 2023; Luhmann et al., 2022; Younas et al., 2022; Palmerio et al., 2022; Bregou et al., 2022; Mlynczak et al., 2022; Varela et al., 2022; Badman et al., 2023; Hewins, Gibson, Webb, et al., 2023 under review; Allen et al., 2023 under review) represent the beginnings of analyses that are likely to continue for years to come.

3.2 Comparative Solar Minima

At first glance, considering Figure 1, it appears that the solar magnetic structure of WHPI was a bit more like WSM than WHI, in that it had a more dipole-type structure with coronal holes centered on the poles. On the other hand, as discussed in Hewins, Gibson, Webb, et al. (2023 under review, a paper in this collection), the extended WHPI period had significant and persistent low-latitude coronal holes that disrupted this simple morphology, similar to what was observed during WHI. As we will discuss further in Section 4, the white light corona during WHPI was not always as dipolar as Figure 1 c). The low-latitude coronal holes were least prevalent in late March 2019 when the observations shown in Figure 1c) were taken, so that it represents the simplest, but not necessarily the typical structure during the WHPI extended interval.

Figure 3 shows the dipole vs quadrupole components of the photospheric magnetic field, showing that the dipole component was strongest during WSM, weakest during WHI, and in the middle during WHPI. This is consistent with the results of Riley et al. (2022, a paper in this collection) who found similar trends in the solar polar magnetic field, which is controlled by the strength of the dipole term. The overall coronal magnetic morphology of closed vs open field is impacted by the ratio of this dipole term relative to higher-

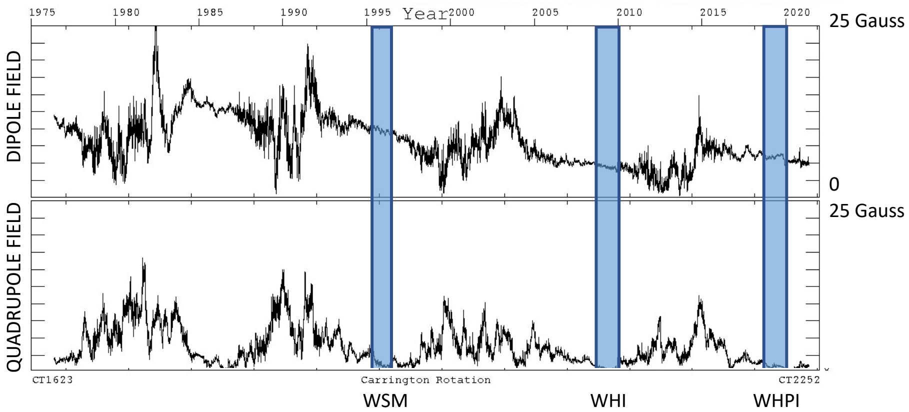

Figure 3. Dipole (top) and quadrupole (bottom) components of the solar photospheric magnetic field, as determined from observations obtained by Stanford's Wilcox Solar Observatory `http://wso.stanford.edu/gifs/Multipole.gif`. The three intervals, WSM, WHI, and WHPI are indicated by the shaded blue rectangles. From this it is clear that the dipolar field was strongest for WSM and weakest for WHI, with WHPI lying in between, but that the quadrupolar field was similar for all three.

order multipole fields. Figure 3 illustrates that the quadrupolar magnetic term is similar in all three intervals, but varies somewhat. In particular, it hits a low during March 2019. Thus, the global coronal magnetic structure as manifested in white-light observations (Figure 1) was predominantly dipolar during the shorter minimum of WSM, never attained that status during the extended minimum of WHI, and demonstrated both white-light dipolar structure and sustained low-latitude coronal holes during the extended WHPI minimum.

These differences of solar dipole strength and coronal magnetic morphology affect the nature of the solar wind near sunspot minimum. Riley et al. (2022) did a statistical comparison of the three solar minima and found, as was the case with the polar magnetic fields, that the WHPI solar wind properties lay in between those of WSM and WHI. Luhmann et al. (2022, a paper in this collection) determined the sources of solar wind velocity measured in the ecliptic from global coronal magnetic models and found that low-to-mid latitude open fields (as opposed to polar open fields) were the primary source of solar wind measured at the Earth, in particular during the extended minima of WHI and WHPI. Thus, to summarize, coronal magnetic field and solar wind observations indicate that WHPI was similar to WHI in its length and magnetic complexity, but demonstrated at least a "partial recovery" of solar dipole dominance and solar wind density and velocity. Thus, WSM > WHPI > WHI in terms of dipole dominance and solar wind properties at solar minimum.

However, the behavior at the Earth paints a somewhat different picture. Once anthropogenic effects (rising CO_2 levels, which cause a secular decrease in thermospheric temperatures) are taken into account, the Earth's upper atmosphere can be a sensitive measure of differences between solar minima. Using measurements of satellite drag, Emmert et al. (2010) found a decrease in thermospheric density ($\sim$ 30% at 400 km) and temperature during the WHI minimum relative to prior minima. (Solomon et al., 2011) conducted model simulations and found a $\sim 27\%$ decrease of annual mean density changes at 400 km altitude from 1996 to 2008. Among this $\sim 27\%$ decrease, $\sim 22\%$, $\sim 2.2\%$, and $\sim 3\%$ were attributed to solar EUV decrease, geomagnetic activity change, and CO_2

increase, respectively. Mlynczak et al. (2022, a paper in this collection) measured a downward trend in thermospheric temperatures from 2002 to 2019 using measurements from the TIMED satellite. After accounting for anthropogenic CO_2 increase, they found temperatures at lower thermospheric altitudes ($10^{-4}hPa$, 105km) had dropped -14.37 K between 2002 and 2019 – and that the lower thermospheric temperatures in the 2019 minimum (WHPI) were $\sim 3K$ colder than the 2008-2009 minimum (WHI). Thus, in terms of thermospheric temperature, WSM < WHI < WHPI, with no sign of the "partial recovery" discussed by Riley et al. (2022).

Relatedly, Bregou et al. (2022, a paper in this collection) found a long-term (1980 to mid-2021) increase in inner zone radiation belt proton flux that they interpreted as a manifestation of the secular downtrend in F10.7 correlated with sunspot number known as the Centennial Gleissberg Cycle (Gleissberg, 1944; Feynman & Ruzmaikin, 2011). F10.7 serves as a proxy for solar EUV in the Bregou et al. study, with a decrease implying a reduced atmospheric (and ionospheric) scale height and reduced collisional drag at a fixed altitude, which is the primary loss mechanism for inner zone protons. Each solar minimum since 1980 has been followed by a maximum trapped proton flux which has shown a secular increase, modulated by the solar cycle, over the past 40 years. Thus, correlated with cooling in the thermosphere, the inner zone radiation belt proton flux has continued to increase with each successive minimum, so WSM < WHI < WHPI — again, no sign of a partial recovery and consistent with a response to the Sun's secular approach to the Gleissberg minimum in solar activity.

To explain the apparent discrepancy between the solar wind and planetary environmental trends, we consider the sometimes competing natures of radiative vs particulate forcing of planetary atmospheres. (Emmert et al., 2010) argued that the decrease in thermospheric densities and temperatures was a result of a decrease in EUV spectral irradiance from the WSM to the WHI solar minimum, and this was supported by the Solomon et al. (2011) modeling study, which found that irradiance changes between WSM and WHI were the dominant cause of the secular trend (relative to particulate and anthropogenic forcings). The case for decreased irradiance being the cause of the ongoing downward trend in thermospheric temperatures from WHI to WHPI is less clear: Using SORCE satellite data from 2003-2020, Woods et al. (2022) found no significant differences in integrated solar spectral irradiance between the two time periods – so, neither a "partial recovery" in irradiance nor a continuing decrease in integrated spectral solar irradiance. However, Mlynczak et al. (2022) argued that when one considered just the narrow Schumann-Runge Bands of solar ultraviolet radiation from 175 to 200 nm, a region responsible for heating of the lower thermosphere, there was a statistically significant decrease in SORCE-measured irradiance between the WHI and WHPI minima. Further modeling is needed to fully understand the causes of the decrease in thermospheric temperatures from WHI to WHPI.

4 Evolution of a Solar Minimum

WHPI spanned the entire solar minimum period between 2018 and 2020. For the purpose of coordinating targeted observations, we identified a few focus "campaign" time periods that took advantage of solar-heliosphere-planetary synergies. These included the solar eclipse in July 2019 – which was studied both for its solar structure (Lloveras et al., 2022, a paper in this collection) and for the Earth's thermospheric response to it as measured by the GOLD satellite (Aryal et al., 2020). They also included the Parker Solar Probe perihelion passage in January 2020 – which served as a template for community coordination and predictive targeting (Badman et al., 2023, a paper in this collection). Beyond that, we trusted to solar serendipity to provide interesting time periods for study, and we were not disappointed!

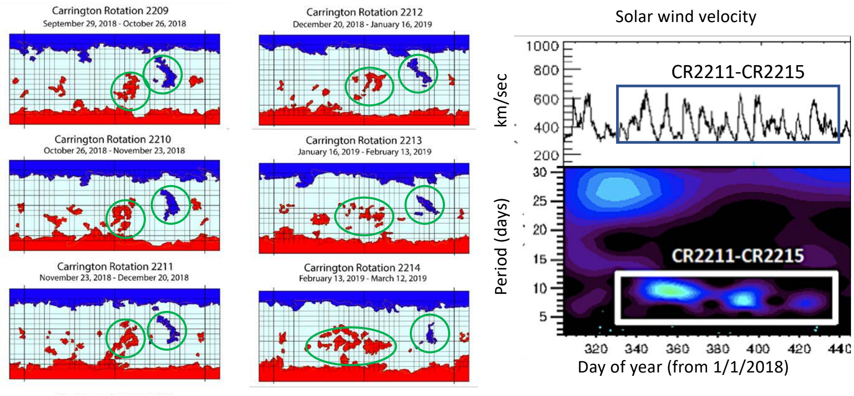

Figure 4. (left and middle columns) McIntosh Archive style Carrington maps (latitude vs. longitude; see Figure 2) for Carrington rotations 2209 through 2214 (September 21 2018 – March 5, 2019; note the ∼27-day solar rotations shown are "padded" on each side by a week of observations), showing long-lived low-latitude coronal holes of both polarities in the right half of maps (green circles). Adapted from Figure 10 of Hewins, Gibson, Webb, et al. (2023 under review). The effects of differential rotation (faster solar rotation at equator than higher latitudes) can be seen in the drift of the equatorial portion of both coronal holes to the right (the equator rotates prograde relative to the synoptic Carrington rate of 27.3 days; see discussion in Luhmann et al. (2022)). (right column) Solar wind at Earth vs time (top) and related wavelet (bottom) showing periodic solar wind 7-9 day forcing. Data from `https://omniweb.gsfc.nasa.gov/`.

4.1 September 2018 - March 2019 – Long-lived low-latitude coronal holes and periodic forcing

Even when solar activity was low, low-latitude coronal holes were present for a significantly long time period. In particular, two coronal holes of opposite polarity separated by approximately 90 degrees remained visible for several rotations (Figure 4 left and middle columns). As discussed in Hewins, Gibson, and Emery (2023 under review), both of these coronal holes resulted in repeating fast wind streams observed at Earth, Mars, and STEREO-A. This 7-9-day periodic solar-wind forcing, shown in Figure 4 right column, is not unlike that observed in the early phases of WSM (Gibson et al., 2010; Emery et al., 2009; Lei et al., 2011), with impact felt in the Earth's upper atmosphere as measured in neutral density by the Swarm-C satellites. Large effects were also registered in the ionosphere through ground-based GNSS total electron content (F. Gasperini, in preparation).

4.2 March 2019 - July 2019: Quiet with a burst of activity in the middle

The interval 2018 – 2020 was a long period of low solar sunspot number and solar magnetic activity, but it was briefly interrupted by a burst of old-cycle sunspot emergence and associated activity in April – June 2019 (Figure 5). This burst of activity resulted in multiple CMEs that erupted from a nest of active regions with impacts measured at both the Earth and Mars (E. Palmerio, private communication). Such events are excellent candidates for studying the evolution of CMEs in the solar wind as a function of distance from their solar origin (Witasse et al., 2017), as well as for considering the relative effects of CMEs vs SIRs on planetary space environments during times of

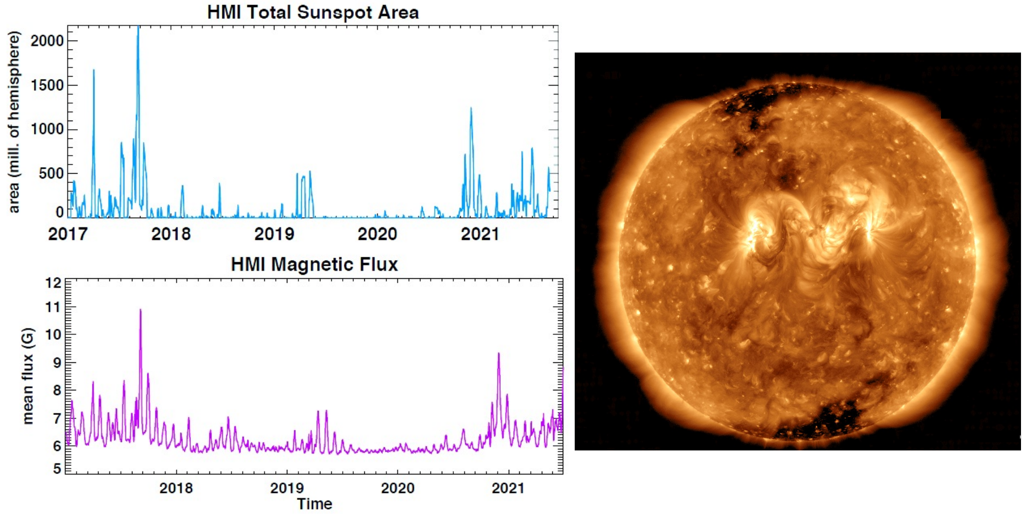

Figure 5. (left) Total sunspot area determined from Solar Dynamics Observatory (SDO) Helioseismic and Magnetic Imager (HMI) intensities (top) and associated magnetic flux (bottom), as a function of time during the WHPI solar minimum. (right) Nest of active regions during (May 12, 2019) which resulted in multiple CMEs detected throughout the solar system (SDO/AIA image, obtained via helioviewer.org)

.

relative heliospheric simplicity (Hudson et al., 2021, a paper in this collection). In an analysis of a series of solar transient events immediately prior to the WHPI time period (August 2018), Palmerio et al. (2022, a paper in this collection) was able to separate out the effects of two CMEs and a following high-speed stream by comparing observations at the Earth and Mars in the context of a global MHD model.

4.3 August - December, 2019: The persistance of "Mr. T"

The long-lived, low-latitude coronal holes of September 2018 - March, 2019 shown in Figure 4 had largely dissipated by April, 2019, in part due to differential rotation of these latitudinally-extended structures and resulting distortion and fragmentation (Hewins, Gibson, Webb, et al., 2023 under review). They were replaced by the active region nest of April-June 2019, which emerged and then decayed, to be replaced in turn by a new positive-polarity (blue) coronal hole that survived for approximately six months (Figure 6; see also Figure 2)).

This coronal hole was extremely geoeffective, perhaps due to its 'T' shape which meant that, near the equator, it was both wide in longitude (and so driving a longer-lasting fast wind stream in time), and tall in latitude (increasing the likelihood of the Earth being repeatedly hit by at least part of its stream). In early September, the sustained fast wind resulted in a radiation belt response that was the highest energy (hardest relativistic electron spectrum) observed in the last two years of the Van Allen Probes mission (Mauk et al., 2013). The radiation-belt response to the CIR lasted into October 2019 and was higher than the response seen during the CME events associated with the active region nest of May 2019 (Hudson et al., 2021).

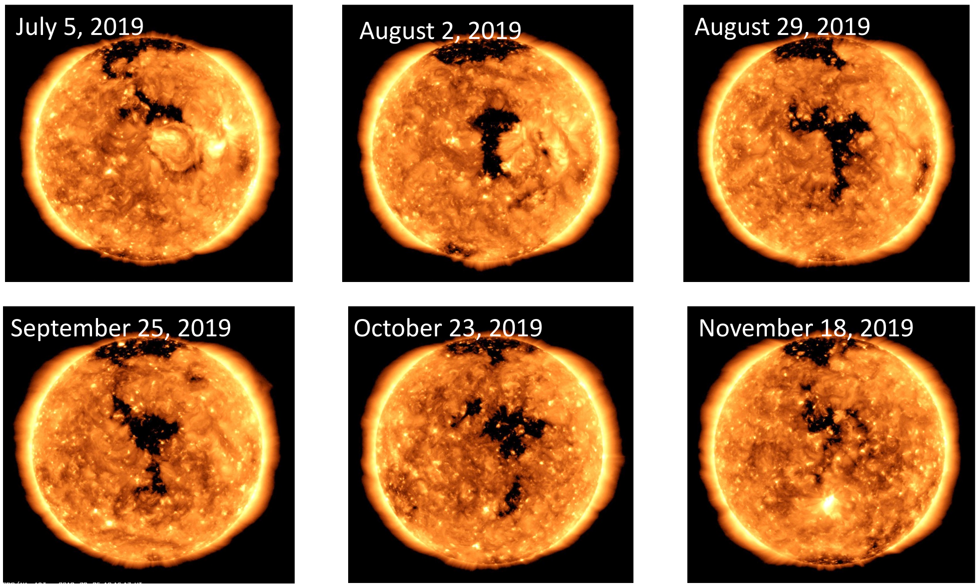

Figure 6. The 'Mr. T' long-lived coronal hole which recurred over six solar Carrington rotations. Shown here in 195 Å as observed by SDO/AIA.

The presence of this long-lived coronal hole at the Sun also overlapped with a time period when Parker Solar Probe was radially aligned with the STEREO-A spacecraft, allowing analyses of the evolution of the associated SIR and a study of energetic particle acceleration (Allen et al., 2021; Wijsen et al., 2021). Measurements of SIRs and CMEs at different longitudinal points in the solar system were also made possible via multi-spacecraft measurements. For a comprehensive overview of this coronal hole and its impacts throughout the heliosphere, see Allen et al. (2023 under review, a paper in this collection).

5 Conclusions

The science enabled by focusing on solar minimum is rich and rewarding. During WSM (1996) and WHI (2008-2009) we gained global understanding about the sources and impacts of solar wind, and new insight about how different solar minimum "quiet times" can be from one another. WHPI (2018-2020) is providing yet more insights into the whole heliospheric system. For example:

- The response to solar-wind and solar-irradiance forcings varies greatly from planet to planet. Analyses of the space-weather impacts that do occur is an excellent way to test our understanding of the coupled mechanisms at play.
- By coronal/solar wind forcing standards, WSM > WHPI > WHI, but radiation-belt and upper atmospheric observations show more of a monotonic secular trend, WSM < WHI < WHPI. This may be due to opposing trends in spectral irradiance vs. solar wind forcing over the past two minima. It illustrates the complexity of understanding system variability when multiple mechanisms – including anthropogenic ones – are involved.

- Multispacecraft/multipoint measurements throughout the heliosphere, varying both in distance and longitude, enable detailed analyses of the evolution of solar wind structures and their sources.

A final comment: with each minimum, observational and modeling capabilities have improved along with data-model interpretation schema. The international interdisciplinary initiatives of WSM, WHI, and WHPI act as catalysts for new analysis approaches and (importantly) play a role in building enduring cohorts of scientific collaborators across scientific disciplines. These efforts should be continued in future minima, as they play an important role in quantifying and understanding long-term changes in the Sun and their effects on the solar wind and planetary space environments and atmospheres.

6 Open Research

GONG magnetic field extrapolations are available at `https://gong.nso.edu/data/magmap/QR/bqg/`.

Mauna Loa Solar Observatory white light coronagraph images are available at `https://mlso.hao.ucar.edu/mlso_data_calendar.php`).

McIntosh archive maps presented in this paper are available through the NOAA National Centers for Environmental Information. doi:10.7289/V5765CCQ. The maps and supplemental reference/methodology materials are archived at `https://www.ngdc.noaa.gov/stp/space-weather/solar-data/solar-imagery/composites/synoptic-maps/mc-intosh/`. Further information on the use and application these data can be found at `https://www2.hao.ucar.edu/mcintosh-archive`.

Additional data appears from the Solar Dynamics Observatory Atmospheric Imaging Assembly (AIA) and Helioseismic and Magnetic Imager (HMI) as accessed through Helioviewer (`https://helioviewer.org/?movieId=hnTN5`). SDO data courtesy of NASA/SDO and the AIA, EVE, and HMI science teams.

Stanford Wilcox Solar Observatory dipole and quadrupole data may be obtained at `http://wso.stanford.edu/#Other`.

Solar wind data are available at `https://omniweb.gsfc.nasa.gov/`.

Acknowledgments

We are indebted to all the participants of the WHPI Workshop of September, 2021. We owe particular thanks to Saurav Aryal, Fran Bagenal, Joan Burkepile, Gina DiBraccio, Heather Elliott, Xiaohua Fang, Rachael Filwett, Dan Gershman, Lan Jian, Janet Kozyra, Christina Lee, Janet Luhmann, Carlos Martinis, Ryan McGranaghan, Marty Mlynczak, Erika Palmerio, Kledsai Poopakun, Nour Raouafi, Pete Riley, Yi-Ming Wang, Nicolas Wijsen, and Olivier Witasse. Funding for SEG, RCA, GdT, BE, IH, and LQ was provided by the NASA HSO Connect program. FG acknowledges support from NASA MDAP Grant No. 80NSSC21K1821. NCAR is a major facility sponsored by the NSF under Cooperative Agreement No. 1852977.

References

Alexander, D. (1999). Temperature structure of the quiet sun x ray corona. *Journal of Geophysical Research: Space Physics*, *104*(A5), 9701-9708. Retrieved from `https://agupubs.onlinelibrary.wiley.com/doi/abs/10.1029/1998JA900016` doi: https://doi.org/10.1029/1998JA900016

Allen, R. C., Gibson, S. E., Hewins, I. M., Vines, S. K., Qian, L., de Toma, G., ... Hill, M. (2023 under review). A Mosaic of the inner heliosphere: Three Carrington rotations during the Whole Heliosphere and Planetary Interactions Interval. . (under review [Paper 2023JA031361])

Allen, R. C., Ho, G. C., Mason, G. M., Li, G., Jian, L. K., Vines, S. K., ... Wiedenbeck, M. (2021, February). Radial Evolution of a CIR: Observations From a Nearly Radially Aligned Event Between Parker Solar Probe and STEREO A. , *48*(3), e91376. doi: 10.1029/2020GL091376

Allen, R. C., Mitchell, D. G., Paranicas, C. P., Hamilton, D. C., Clark, G., Rymer, A. M., ... Vandegriff, J. (2018, June). Internal Versus External Sources of Plasma at Saturn: Overview From Magnetospheric Imaging Investigation/Charge-Energy-Mass Spectrometer Data. *Journal of Geophysical Research (Space Physics)*, *123*(6), 4712-4727. doi: 10.1029/2018JA025262

Altrock, R. C. (2011, December). Coronal Fe XIV Emission During the Whole Heliosphere Interval Campaign. , *274*(1-2), 251-257. doi: 10.1007/s11207-011-9714-9

Araujo-Pradere, E. A., Redmon, R., Fedrizzi, M., Viereck, R., & Fuller-Rowell, T. J. (2011, December). Some Characteristics of the Ionospheric Behavior During the Solar Cycle 23 - 24 Minimum. , *274*(1-2), 439-456. doi: 10.1007/s11207-011-9728-3

Aryal, S., Evans, J. S., Correira, J., Burns, A. G., Wang, W., Solomon, S. C., ... Jee, G. (2020, September). First Global-Scale Synoptic Imaging of Solar Eclipse Effects in the Thermosphere. *Journal of Geophysical Research (Space Physics)*, *125*(9), e27789. doi: 10.1029/2020JA027789

Badman, S. T., Riley, P., Jones, S. I., Kim, T. K., Allen, R. C., Arge, C. N., ... Verniero, J. L. (2023). Prediction and verification of Parker Solar Probe solar wind sources. at 13.3 Rsun. . doi: 10.1029/2023JA031359

Bagenal, F. (2013). Planetary Magnetospheres. In T. D. Oswalt, L. M. French, & P. Kalas (Eds.), *Planets, stars and stellar systems. volume 3: Solar and stellar planetary systems* (p. 251). doi: 10.1007/978-94-007-5606-9_6

Bagenal, F., & Dols, V. (2020, May). The Space Environment of Io and Europa. *Journal of Geophysical Research (Space Physics)*, *125*(5), e27485. doi: 10.1029/2019JA027485

Benito, J., Kuo, P.-C., Widrig, K. E., Jagt, J. W. M., & Field, D. J. (2022, December). Cretaceous ornithurine supports a neognathous crown bird ancestor. , *612*(7938), 100-105. doi: 10.1038/s41586-022-05445-y

Biesecker, D. A., Thompson, B. J., Gibson, S. E., Flucra, A., Gopalswamy, N., Hoeksema, J. T., ... Strachan, L. (1999). Synoptic sun during the first whole sun month campaign: August 10 to september 8, 1996. *Journal of Geophysical Research: Space Physics*, *104*(A5), 9679-9689. Retrieved from `https://agupubs.onlinelibrary.wiley.com/doi/abs/10.1029/1998JA900056` doi: https://doi.org/10.1029/1998JA900056

Bingham, S. T., Mouikis, C. G., Kistler, L. M., Boyd, A. J., Paulson, K., Farrugia, C. J., ... Kletzing, C. (2018, December). The Outer Radiation Belt Response to the Storm Time Development of Seed Electrons and Chorus Wave Activity During CME and CIR Driven Storms. *Journal of Geophysical Research (Space Physics)*, *123*(12), 10,139-10,157. doi: 10.1029/2018JA025963

Bisi, M. M., Jackson, B. V., Buffington, A., Clover, J. M., Hick, P. P., & Tokumaru, M. (2009, May). Low-Resolution STELab IPS 3D Reconstructions of the Whole Heliosphere Interval and Comparison with in-Ecliptic Solar Wind Measurements from STEREO and Wind Instrumentation. , *256*(1-2), 201-217. doi: 10.1007/s11207-009-9350-9

Bisi, M. M., Jackson, B. V., Fallows, R. A., Dorrian, G. D., Manoharan, P. K., Clover, J. M., ... Tokumaru, M. (2010, May). Solar Wind and CME Studies of the Inner Heliosphere Using IPS Data from Stelab, ORT, and EISCAT. In *Advances in geosciences, volume 21: Solar terrestrial (st)* (Vol. 21, p. 33-49). doi: 10.1142/9789812838209_0003

Bisi, M. M., Thompson, B. J., Emery, B. A., Gibson, S. E., Leibacher, J., & van Driel-Gesztelyi, L. (2011, December). The Sun-Earth Connection near Solar Minimum: Placing it into Context. , *274*(1-2), 1-3. doi: 10.1007/s11207-011-9915-2
Blanc, M., Andrews, D. J., Coates, A. J., Hamilton, D. C., Jackman, C. M., Jia, X., ... Westlake, J. H. (2015, October). Saturn Plasma Sources and Associated Transport Processes. , *192*(1-4), 237-283. doi: 10.1007/s11214-015-0172-9
Borovsky, J. E., & Denton, M. H. (2006, July). Differences between CME-driven storms and CIR-driven storms. *Journal of Geophysical Research (Space Physics)*, *111*(A7), A07S08. doi: 10.1029/2005JA011447
Bougher, S. W., Engel, S., Roble, R. G., & Foster, B. (2000, July). Comparative terrestrial planet thermospheres 3. Solar cycle variation of global structure and winds at solstices. , *105*(E7), 17669-17692. doi: 10.1029/1999JE001232
Bougher, S. W., Pawlowski, D., Bell, J. M., Nelli, S., McDunn, T., Murphy, J. R., ... Ridley, A. (2015, February). Mars Global Ionosphere-Thermosphere Model: Solar cycle, seasonal, and diurnal variations of the Mars upper atmosphere. *Journal of Geophysical Research (Planets)*, *120*(2), 311-342. doi: 10.1002/2014JE004715
Breen, A. R., Mikic, Z., Linker, J. A., Lazarus, A. J., Thompson, B. J., Biesecker, D. A., ... Lecinski, A. (1999). Interplanetary scintillation measurements of the solar wind during whole sun month: Comparisons with coronal and in situ observations. *Journal of Geophysical Research: Space Physics*, *104*(A5), 9847-9870. Retrieved from `https://agupubs.onlinelibrary.wiley.com/doi/abs/10.1029/1998JA900091` doi: https://doi.org/10.1029/1998JA900091
Breen, A. R., Thompson, B. J., Kojima, M., Biesecker, D. A., Canals, A., Fallows, R. A., ... Williams, P. J. S. (2000, November). Measurements of the solar wind over a wide range of heliocentric distances - a comparison of results from the first three Whole Sun Months. *Journal of Atmospheric and Solar-Terrestrial Physics*, *62*(16), 1527-1543. doi: 10.1016/S1364-6826(00)00090-0
Bregou, E. J., Hudson, M. K., Kress, B. T., Qin, M., & Selesnick, R. S. (2022, July). Gleissberg Cycle Dependence of Inner Zone Proton Flux. *Space Weather*, *20*(7), e2022SW003072. doi: 10.1029/2022SW003072
Bromage, B. J. J., Alexander, D., Breen, A., Clegg, J. R., Del Zanna, G., DeForest, C., ... Browning, P. K. (2000, April). Structure of a Large low-Latitude Coronal Hole. , *193*, 181-193. doi: 10.1023/A:1005209725885
Bruntz, R., Lopez, R. E., Bhattarai, S. K., Pham, K. H., Deng, Y., Huang, Y., ... Lyon, J. G. (2012, July). Investigating the viscous interaction and its role in generating the ionospheric potential during the Whole Heliosphere Interval. *Journal of Atmospheric and Solar-Terrestrial Physics*, *83*, 70-78. doi: 10.1016/j.jastp.2012.03.016
Candido, C. M. N., Batista, I. S., Klausner, V., de Siqueira Negreti, P. M., Becker-Guedes, F., de Paula, E. R., ... Correia, E. S. (2018, June). Response of the total electron content at Brazilian low latitudes to corotating interaction region and high-speed streams during solar minimum 2008. *Earth, Planets and Space*, *70*(1), 104. doi: 10.1186/s40623-018-0875-8
Chadney, J. M., Koskinen, T. T., Hu, X., Galand, M., Lavvas, P., Unruh, Y. C., ... Yelle, R. V. (2022, January). Energy deposition in Saturn's equatorial upper atmosphere. , *372*, 114724. doi: 10.1016/j.icarus.2021.114724
Chamberlin, P. C., Woods, T. N., Crotser, D. A., Eparvier, F. G., Hock, R. A., & Woodraska, D. L. (2009, March). Solar cycle minimum measurements of the solar extreme ultraviolet spectral irradiance on 14 April 2008. , *36*(5), L05102. doi: 10.1029/2008GL037145
Clegg, J. R., Bromage, B. J. I., & Browning, P. K. (1999). Modeling the coronal magnetic field, with a new method for obtaining boundary conditions on the farside of the sun. *Journal of Geophysical Research: Space Physics*,

104 (A5), 9831-9846. Retrieved from https://agupubs.onlinelibrary.wiley.com/doi/abs/10.1029/1998JA900149 doi: https://doi.org/10.1029/1998JA900149

Cremades, H., Mandrini, C. H., & Dasso, S. (2011, December). Coronal Transient Events During Two Solar Minima: Their Solar Source Regions and Interplanetary Counterparts. , *274* (1-2), 233-249. doi: 10.1007/s11207-011-9769-7

de Toma, G. (2011, December). Evolution of Coronal Holes and Implications for High-Speed Solar Wind During the Minimum Between Cycles 23 and 24. , *274* (1-2), 195-217. doi: 10.1007/s11207-010-9677-2

Del Zanna, G., Gibson, S. E., Mason, H. E., Pike, C. D., & Mandrini, C. H. (2002, January). Sigmoidal diagnostics with SOHO/CDS. *Advances in Space Research*, *30* (3), 551-556. doi: 10.1016/S0273-1177(02)00341-1

Delamere, P. A., & Bagenal, F. (2010, October). Solar wind interaction with Jupiter's magnetosphere. *Journal of Geophysical Research (Space Physics)*, *115* (A10), A10201. doi: 10.1029/2010JA015347

Delamere, P. A., & Bagenal, F. (2013, November). Magnetotail structure of the giant magnetospheres: Implications of the viscous interaction with the solar wind. *Journal of Geophysical Research (Space Physics)*, *118* (11), 7045-7053. doi: 10.1002/2013JA019179

Delamere, P. A., Bagenal, F., Dols, V., & Ray, L. C. (2007, May). Saturn's neutral torus versus Jupiter's plasma torus. , *34* (9), L09105. doi: 10.1029/2007GL029437

Del Zanna, G., & Bromage, B. J. I. (1999). The elephant's trunk: Spectroscopic diagnostics applied to soho/cds observations of the august 1996 equatorial coronal hole. *Journal of Geophysical Research: Space Physics*, *104* (A5), 9753-9766. Retrieved from https://agupubs.onlinelibrary.wiley.com/doi/abs/10.1029/1998JA900067 doi: https://doi.org/10.1029/1998JA900067

Dobrzycka, D., Cranmer, S. R., Panasyuk, A. V., Strachan, L., & Kohl, J. L. (1999). Study of the latitudinal dependence of h i lyman and o vi emission in the solar corona: Evidence for the superradial geometry of the outflow in the polar coronal holes. *Journal of Geophysical Research: Space Physics*, *104* (A5), 9791-9799. Retrieved from https://agupubs.onlinelibrary.wiley.com/doi/abs/10.1029/1998JA900129 doi: https://doi.org/10.1029/1998JA900129

Dungey, J. W. (1961, January). Interplanetary Magnetic Field and the Auroral Zones. , *6* (2), 47-48. doi: 10.1103/PhysRevLett.6.47

Echer, E., Tsurutani, B. T., Gonzalez, W. D., & Kozyra, J. U. (2011, December). High Speed Stream Properties and Related Geomagnetic Activity During the Whole Heliosphere Interval (WHI): 20 March to 16 April 2008. , *274* (1-2), 303-320. doi: 10.1007/s11207-011-9739-0

Edberg, N. J. T., Nilsson, H., Futaana, Y., Stenberg, G., Lester, M., Cowley, S. W. H., … Zhang, T. L. (2011, September). Atmospheric erosion of Venus during stormy space weather. *Journal of Geophysical Research (Space Physics)*, *116* (A9), A09308. doi: 10.1029/2011JA016749

Eiscat, Ort, & Data, N. (2000, September). Observations of interplanetary scintillation during the 1998 Whole Sun Month: a comparison between. *Annales Geophysicae*, *18* (9), 1003-1008. doi: 10.5194/angeo-18-1003-2000

Emery, B. A., Richardson, I. G., Evans, D. S., Rich, F. J., & Wilson, G. R. (2011, December). Solar Rotational Periodicities and the Semiannual Variation in the Solar Wind, Radiation Belt, and Aurora. , *274* (1-2), 399-425. doi: 10.1007/s11207-011-9758-x

Emery, B. A., Richardson, I. G., Evans, D. S., Rich, F. J., & Xu, W. (2009). Solar wind structure sources and periodicities of global electron hemispheric power over three solar cycles. *Journal of Atmospheric and Solar-Terrestrial Physics*. doi: 10.1016/j.jastp.2008.08.005

Emmert, J. T., Lean, J. L., & Picone, J. M. (2010). Anomalously low solar extreme-ultraviolet irradiance and thermospheric density during solar minimum. *Geophys. Res. Lett.*, *37*.

Fang, X., Forbes, J. M., Benna, M., Montabone, L., Curry, S., & Jakosky, B. (2022, March). The Origins of Long-Term Variability in Martian Upper Atmospheric Densities. *Journal of Geophysical Research (Space Physics)*, *127*(3), e30145. doi: 10.1029/2021JA030145

Feynman, J., & Ruzmaikin, A. (2011, September). The Sun's Strange Behavior: Maunder Minimum or Gleissberg Cycle? , *272*(2), 351. doi: 10.1007/s11207-011-9828-0

Fludra, A., Del Zanna, G., Alexander, D., & Bromage, B. J. I. (1999). Electron density and temperature of the lower solar corona. *Journal of Geophysical Research: Space Physics*, *104*(A5), 9709-9720. Retrieved from `https://agupubs.onlinelibrary.wiley.com/doi/abs/10.1029/1998JA900033` doi: https://doi.org/10.1029/1998JA900033

Frazin, R. A., & Janzen, P. (2002, May). Tomography of the Solar Corona. II. Robust, Regularized, Positive Estimation of the Three-dimensional Electron Density Distribution from LASCO-C2 Polarized White-Light Images. , *570*(1), 408-422. doi: 10.1086/339572

Galvin, A. B., & Kohl, J. L. (1999). Whole sun month at solar minimum: An introduction. *Journal of Geophysical Research: Space Physics*, *104*(A5), 9673-9678. Retrieved from `https://agupubs.onlinelibrary.wiley.com/doi/abs/10.1029/1999JA900008` doi: https://doi.org/10.1029/1999JA900008

Gasperini, F., Hughes, J., & Thiemann, E. M. B. (2023, January). Solar Rotation Effects in Earth's and Mars' Thermospheric Densities as Revealed by Concurrent MAVEN, Swarm-C, and GOES Observations. *Journal of Geophysical Research (Planets)*, *128*(1), e2022JE007431. doi: 10.1029/2022JE007431

Gershman, D. J., & DiBraccio, G. A. (2020, December). Solar Cycle Dependence of Solar Wind Coupling With Giant Planet Magnetospheres. , *47*(24), e89315. doi: 10.1029/2020GL089315

Gibson, S. E. (2001, May). Global Solar Wind Structure from Solar Minimum to Solar Maximum: Sources and Evolution. , *97*, 69-79. doi: 10.1023/A:1011869926351

Gibson, S. E., Biesecker, D., Guhathakurta, M., Hoeksema, J. T., Lazarus, A. J., Linker, J., . . . Zhao, X. P. (1999, August). The Three-dimensional Coronal Magnetic Field during Whole Sun Month. , *520*(2), 871-879. doi: 10.1086/307496

Gibson, S. E., de Toma, G., Emery, B., Riley, P., Zhao, L., Elsworth, Y., . . . Webb, D. (2011, December). The Whole Heliosphere Interval in the Context of a Long and Structured Solar Minimum: An Overview from Sun to Earth. , *274*(1-2), 5-27. doi: 10.1007/s11207-011-9921-4

Gibson, S. E., Fletcher, L., Del Zanna, G., Pike, C. D., Mason, H. E., Mandrini, C. H., . . . Thompson, B. J. (2002, August). The Structure and Evolution of a Sigmoidal Active Region. , *574*(2), 1021-1038. doi: 10.1086/341090

Gibson, S. E., Fludra, A., Bagenal, F., Biesecker, D., Del Zanna, G., & Bromage, B. (1999). Solar minimum streamer densities and temperatures using whole sun month coordinated data sets. *Journal of Geophysical Research: Space Physics*, *104*(A5), 9691-9699. Retrieved from `https://agupubs.onlinelibrary.wiley.com/doi/abs/10.1029/98JA02681` doi: https://doi.org/10.1029/98JA02681

Gibson, S. E., Kozyra, J. U., de Toma, G., Emery, B. A., Onsager, T., & Thompson, B. J. (2009, September). If the Sun is so quiet, why is the Earth ringing? A comparison of two solar minimum intervals. *Journal of Geophysical Research (Space Physics)*, *114*(A9), A09105. doi: 10.1029/2009JA014342

Gibson, S. E., Kucera, T. A., Rastawicki, D., Dove, J., de Toma, G., Hao, J., . . . Zhang, M. (2010). Three-dimensional morphology of a coronal prominence cavity. *Astrophys. J.*, *723*, 1133.

Gibson, S. E., Webb, D., Hewins, I. M., McFadden, R. H., Emery, B. A., Denig, W., & McIntosh, P. S. (2017). Beyond sunspots: Studies using the McIntosh Archive of global solar magnetic field patterns. In D. Nandy, A. Valio, & P. Petit (Eds.), *Living around active stars* (Vol. 328, p. 93). Cambridge University Press: Cambridge.

Gleissberg, W. (1944, January). a Table of Secular Variations of the Solar Cycle. *Terrestrial Magnetism and Atmospheric Electricity*, *49*(4), 243-244. doi: 10.1029/TE049i004p00243

Gopalswamy, N., Shibasaki, N., Thompson, B. J., Gurman, J., & DeForest, C. (1999). Microwave enhancement and variability in the elephant's trunk coronal hole: Comparison with soho observations. *Journal of Geophysical Research: Space Physics*, *104*(A5), 9767-9779. Retrieved from `https://agupubs.onlinelibrary.wiley.com/doi/abs/10.1029/1998JA900168` doi: https://doi.org/10.1029/1998JA900168

Guhathakurta, M., Fludra, A., Gibson, S. E., Biesecker, D., & Fisher, R. (1999). Physical properties of a coronal hole from a coronal diagnostic spectrometer, mauna loa coronagraph, and lasco observations during the whole sun month. *Journal of Geophysical Research: Space Physics*, *104*(A5), 9801-9808. Retrieved from `https://agupubs.onlinelibrary.wiley.com/doi/abs/10.1029/1998JA900082` doi: https://doi.org/10.1029/1998JA900082

Guhathakurta, M., Sittler, E. C., & Ofman, L. (2006, November). Semiempirically derived heating function of the corona heliosphere during the Whole Sun Month. *Journal of Geophysical Research (Space Physics)*, *111*(A11), A11215. doi: 10.1029/2006JA011931

Haberreiter, M. (2011, December). Solar EUV Spectrum Calculated for Quiet Sun Conditions. , *274*(1-2), 473-479. doi: 10.1007/s11207-011-9767-9

Hathaway, D. H. (2015, September). The Solar Cycle. *Living Reviews in Solar Physics*, *12*, 4. doi: 10.1007/lrsp-2015-4

Hewins, I. M., Gibson, S. E., & Emery, B. A. (2023 under review). WHPI Synoptic Coronal hole maps and solar wind studies. . (under review)

Hewins, I. M., Gibson, S. E., Webb, D. F., McFadden, R. H., A., K. T., & Emery, B. A. (2023 under review). Comparative Solar Minima using the McIntosh Archive. . (Paper under review, [Paper 2023JA031343])

Hewins, I. M., Gibson, S. E., Webb, D. F., McFadden, R. H., A., K. T., Emery, B. A., & McIntosh, S. W. (2020). The Evolution of Coronal Holes over Three Solar Cycles Using the McIntosh Archive. , *295*, 161. doi: 10.1007/s11207-020-01731-y

Hudson, M., Brito, T., Elkington, S., Kress, B., Li, Z., & Wiltberger, M. (2012, July). Radiation belt 2D and 3D simulations for CIR-driven storms during Carrington Rotation 2068. *Journal of Atmospheric and Solar-Terrestrial Physics*, *83*, 51-62. doi: 10.1016/j.jastp.2012.03.017

Hudson, M. K., Elkington, S. R., Li, Z., Patel, M., Pham, K., Sorathia, K., ... Leali, A. (2021, December). MHD-Test Particles Simulations of Moderate CME and CIR-Driven Geomagnetic Storms at Solar Minimum. *Space Weather*, *19*(12), e02882. doi: 10.1029/2021SW002882

Hughes, J., Gasperini, F., & Forbes, J. M. (2022, January). Solar Rotation Effects in Martian Thermospheric Density as Revealed by Five Years of MAVEN Observations. *Journal of Geophysical Research (Planets)*, *127*(1), e07036. doi: 10.1029/2021JE007036

Jackman, C. M., & Arridge, C. S. (2011, December). Solar Cycle Effects on the Dynamics of Jupiter's and Saturn's Magnetospheres. , *274*(1-2), 481-502. doi: 10.1007/s11207-011-9748-z

Jakosky, B. M., Grebowsky, J. M., Luhmann, J. G., Connerney, J., Eparvier, F., Ergun, R., ... Yelle, R. (2015, November). MAVEN observations of the response of Mars to an interplanetary coronal mass ejection. *Science*, *350*(6261), 0210. doi: 10.1126/science.aad0210

Jian, L., Russell, C. T., Luhmann, J. G., & Skoug, R. M. (2006, December). Properties of Stream Interactions at One AU During 1995 2004. , *239*(1-2), 337-392. doi: 10.1007/s11207-006-0132-3

Ko, Y. K., Raymond, J. C., Gibson, S. E., Alexander, D., Strachan, L., Holzer, T., ... Fletcher, L. (2005, April). Multialtitude Observations of a Coronal Jet during the Third Whole Sun Month Campaign. , *623*(1), 519-539. doi: 10.1086/428479

Lean, J. (1997, January). The Sun's Variable Radiation and Its Relevance For Earth. , *35*, 33-67. doi: 10.1146/annurev.astro.35.1.33

Lean, J. L., McDonald, S. E., Huba, J. D., Emmert, J. T., Drob, D. P., & Siefring, C. L. (2014, May). Geospace variability during the 2008-2009 Whole Heliosphere Intervals. *Journal of Geophysical Research (Space Physics)*, *119*(5), 3755-3776. doi: 10.1002/2013JA019485

Lee, C. O., Hara, T., Halekas, J. S., Thiemann, E., Chamberlin, P., Eparvier, F., ... Jakosky, B. M. (2017, March). MAVEN observations of the solar cycle 24 space weather conditions at Mars. *Journal of Geophysical Research (Space Physics)*, *122*(3), 2768-2794. doi: 10.1002/2016JA023495

Lei, J., Thayer, J. P., Wang, W., & McPherron, R. L. (2011, December). Impact of CIR Storms on Thermosphere Density Variability during the Solar Minimum of 2008. , *274*(1-2), 427-437. doi: 10.1007/s11207-010-9563-y

Lepping, R. P., Wu, C. C., Berdichevsky, D. B., & Szabo, A. (2011, December). Magnetic Clouds at/near the 2007 - 2009 Solar Minimum: Frequency of Occurrence and Some Unusual Properties. , *274*(1-2), 345-360. doi: 10.1007/s11207-010-9646-9

Li, X., Schiller, Q., Blum, L., Califf, S., Zhao, H., Tu, W., ... Spence, H. (2013, October). First results from CSSWE CubeSat: Characteristics of relativistic electrons in the near-Earth environment during the October 2012 magnetic storms. *Journal of Geophysical Research (Space Physics)*, *118*(10), 6489-6499. doi: 10.1002/2013JA019342

Li, Z., Hudson, M., & Chen, Y. (2014, March). Radial diffusion comparing a THEMIS statistical model with geosynchronous measurements as input. *Journal of Geophysical Research (Space Physics)*, *119*(3), 1863-1873. doi: 10.1002/2013JA019320

Lin, C.-H., & Chen, J. (2015, January). A Comparison of Coronal Mass Ejection Models with Observations for Two Large CMEs Detected During the Whole Heliosphere Interval. *Terrestrial, Atmospheric and Oceanic Sciences*, *26*(2-1), 121. doi: 10.3319/TAO.2014.10.15.01(AA)

Linker, J. A., Mikic, Z., Biesecker, D. A., Forsyth, R. J., E., G. S., Lazarus, A. J., ... Thompson, B. J. (1999). Magnetohydrodynamic modeling of the solar corona during whole sun month. *Journal of Geophysical Research: Space Physics*, *104*(A5), 9809-9830. Retrieved from `https://agupubs.onlinelibrary.wiley.com/doi/abs/10.1029/1998JA900159` doi: https://doi.org/10.1029/1998JA900159

Lionello, R., Linker, J. A., & Mikić, Z. (2009, January). Multispectral Emission of the Sun During the First Whole Sun Month: Magnetohydrodynamic Simulations. , *690*(1), 902-912. doi: 10.1088/0004-637X/690/1/902

Lloveras, D. G., Vásquez, A. M., Nuevo, F. A., Frazin, R. A., Manchester, W., Sachdeva, N., ... Gilardy, H. (2022, June). Three-Dimensional Structure of the Corona During WHPI Campaign Rotations CR-2219 and CR-2223. *Journal of Geophysical Research (Space Physics)*, *127*(6), e30406. doi: 10.1029/2022JA030406

Lopez, R. E., Bhattarai, S. K., Bruntz, R., Pham, K., Wiltberger, M., Lyon, J. G., ... Huang, Y. (2012, July). The role of dayside merging in generating the ionospheric potential during the Whole Heliospheric Interval. *Journal of Atmospheric and Solar-Terrestrial Physics*, *83*, 63-69. doi: 10.1016/j.jastp.2012.03.001

Luhmann, J. G., Fedorov, A., Barabash, S., Carlsson, E., Futaana, Y., Zhang, T. L., ... Brain, D. A. (2008, August). Venus Express observations of atmospheric oxygen escape during the passage of several coronal mass ejections. *Journal of Geophysical Research (Planets)*, *113*(52), E00B04. doi: 10.1029/2008JE003092

Luhmann, J. G., Kasprzak, W. T., & Russell, C. T. (2007, April). Space weather at Venus and its potential consequences for atmosphere evolution. *Journal of Geophysical Research (Planets)*, *112*(E4), E04S10. doi: 10.1029/2006JE002820

Luhmann, J. G., Li, Y., Lee, C. O., Jian, L. K., Arge, C. N., & Riley, P. (2022, October). Solar Cycle Variability in Coronal Holes and Their Effects on Solar Wind Sources. *Space Weather*, *20*(10), e2022SW003110. doi: 10.1029/2022SW003110

Mauk, B. H., Fox, N. J., Kanekal, S. G., Kessel, R. L., Sibeck, D. G., & Ukhorskiy, A. (2013, November). Science Objectives and Rationale for the Radiation Belt Storm Probes Mission. , *179*(1-4), 3-27. doi: 10.1007/s11214-012-9908-y

McComas, D. J., & Bagenal, F. (2007, October). Jupiter: A fundamentally different magnetospheric interaction with the solar wind. , *34*(20), L20106. doi: 10.1029/2007GL031078

McComas, D. J., Bame, S. J., Barraclough, B. L., Feldman, W. C., Funsten, H. O., Gosling, J. T., ... Neugebauer, M. (1998). Ulysses' return to the slow solar wind. *Geophys. Res. Lett.*, *25*, 1-4. doi: 10.1029/97GL03444

McComas, D. J., Elliott, H. A., Schwadron, N. A., Gosling, J. T., Skoug, R. M., & Goldstein, B. E. (2003, May). The three-dimensional solar wind around solar maximum. *Geophys. Res. Lett.*, *30*, 1517. doi: 10.1029/2003GL017136

Mewaldt, R. A., Davis, A. J., L., K. A., L., A., R., Stone, E. C., ... von Rosenvinge, T. T. (2010). Record-setting cosmic-ray intensities in 2009 and 201. *Astrophys. J. Lett.*, *723*, 1.

Millan, R. M., & Thorne, R. M. (2007, March). Review of radiation belt relativistic electron losses. *Journal of Atmospheric and Solar-Terrestrial Physics*, *69*(3), 362-377. doi: 10.1016/j.jastp.2006.06.019

Mlynczak, M. G., Hunt, L. A., Garcia, R. R., Harvey, V. L., Marshall, B. T., Yue, J., ... Russell, J. M. (2022, November). Cooling and Contraction of the Mesosphere and Lower Thermosphere From 2002 to 2021. *Journal of Geophysical Research (Atmospheres)*, *127*(22), e2022JD036767. doi: 10.1029/2022JD036767

Moran, P. J., Ananthakrishnan, S., Balasubramanian, V., Breen, A. R., Canals, A., Fallows, R. A., ... Williams, P. J. S. (2000, September). Observations of interplanetary scintillation during the 1998 Whole Sun Month: a comparison between EISCAT, ORT and Nagoya data. *Annales Geophysicae*, *18*(9), 1003. doi: 10.1007/s00585-000-1003-0

Muller, R., Utz, D., & Hanslmeier, A. (2011, December). Non-Varying Granulation and Photospheric Network During the Extended 2007 - 2009 Solar Minimum. , *274*(1-2), 87-97. doi: 10.1007/s11207-011-9725-6

Nitta, N. V. (2011, December). Observables Indicating Two Major Coronal Mass Ejections During the WHI. , *274*(1-2), 219-232. doi: 10.1007/s11207-011-9806-6

Ogawa, Y., Seki, K., Keika, K., & Ebihara, Y. (2019, May). Characteristics of CME- and CIR-Driven Ion Upflows in the Polar Ionosphere. *Journal of Geophysical Research (Space Physics)*, *124*(5), 3637-3649. doi: 10.1029/2018JA025870

Palmerio, E., Lee, C. O., Richardson, I. G., Nieves-Chinchilla, T., Dos Santos, L. F. G., Gruesbeck, J. R., ... Luhmann, J. G. (2022, September). CME

Evolution in the Structured Heliosphere and Effects at Earth and Mars During Solar Minimum. *Space Weather*, *20*(9), e2022SW003215. doi: 10.1029/2022SW003215

Panasyuk, A. (1999). Three-dimensional reconstruction of uv emissivities in the solar corona using ultraviolet coronagraph spectrometer data from the whole sun month. *Journal of Geophysical Research: Space Physics*, *104*(A5), 9721-9726. Retrieved from `https://agupubs.onlinelibrary.wiley.com/doi/abs/10.1029/1998JA900118` doi: https://doi.org/10.1029/1998JA900118

Petrie, G. J. D., Canou, A., & Amari, T. (2011, December). Nonlinear Force-Free and Potential-Field Models of Active-Region and Global Coronal Fields during the Whole Heliosphere Interval. , *274*(1-2), 163-194. doi: 10.1007/s11207-010-9687-0

Pizzo, V. (1978, December). A three-deminsional model of corotating streams in the solar wind 1. Theoretical foundations. , *83*(A12), 5563-5572. doi: 10.1029/JA083iA12p05563

Poopakun, K., Nuntiyakul, W., Ruffolo, D., Evenson, P., Peng, J., Chuanraksasat, P., ... Oh, S. (2022, March). Solar magnetic polarity effect on neutron monitor count rates from latitude surveys versus Antarctic stations. In *37th international cosmic ray conference* (p. 1268). doi: 10.22323/1.395.01268

Posner, A., Bothmer, V., Thompson, B. J., Kunow, H., Heber, B., Mueller-Mellin, R., ... Linker, J. A. (1999). In-ecliptic cir-associated energetic particle events and polar coronal hole structures: Soho/costep observations for the whole sun month campaign. *Journal of Geophysical Research: Space Physics*, *104*(A5), 9881-9890. Retrieved from `https://agupubs.onlinelibrary.wiley.com/doi/abs/10.1029/98JA02654` doi: https://doi.org/10.1029/98JA02654

Potgieter, M. S. (2013, June). Solar Modulation of Cosmic Rays. *Living Reviews in Solar Physics*, *10*(1), 3. doi: 10.12942/lrsp-2013-3

Riley, P., Caplan, R. M., Downs, C., Linker, J. A., & Lionello, R. (2022, August). Comparing and Contrasting the Properties of the Inner Heliosphere for the Three Most Recent Solar Minima. *Journal of Geophysical Research (Space Physics)*, *127*(8), e30261. doi: 10.1029/2022JA030261

Riley, P., Downs, C., Linker, J. A., Mikic, Z., Lionello, R., & Caplan, R. M. (2019, April). Predicting the Structure of the Solar Corona and Inner Heliosphere during Parker Solar Probe's First Perihelion Pass. , *874*(2), L15. doi: 10.3847/2041-8213/ab0ec3

Riley, P., Gosling, J. T., McComas, D. J., Pizzo, V. J., Luhmann, J. G., Biesecker, D., ... Thompson, B. J. (1999). Relationship between ulysses plasma observations and solar observations during the whole sun month campaign. *Journal of Geophysical Research: Space Physics*, *104*(A5), 9871-9879. Retrieved from `https://agupubs.onlinelibrary.wiley.com/doi/abs/10.1029/1998JA900078` doi: https://doi.org/10.1029/1998JA900078

Riley, P., Linker, J. A., & Mikić, Z. (2001, August). An empirically-driven global MHD model of the solar corona and inner heliosphere. , *106*(A8), 15889-15902. doi: 10.1029/2000JA000121

Riley, P., Lionello, R., Linker, J. A., Mikic, Z., Luhmann, J., & Wijaya, J. (2011, December). Global MHD Modeling of the Solar Corona and Inner Heliosphere for the Whole Heliosphere Interval. , *274*(1-2), 361-377. doi: 10.1007/s11207-010-9698-x

Schwadron, N. A., Rahmanifard, F., Wilson, J., Jordan, A. P., Spence, H. E., Joyce, C. J., ... Zeitlin, C. (2018, March). Update on the Worsening Particle Radiation Environment Observed by CRaTER and Implications for Future Human Deep-Space Exploration. *Space Weather*, *16*(3), 289-303. doi: 10.1002/2017SW001803

Slavin, J. A., Middleton, H. R., Raines, J. M., Jia, X., Zhong, J., Sun, W. J., ... Mays, M. L. (2019, August). MESSENGER Observations of Disappearing

Dayside Magnetosphere Events at Mercury. *Journal of Geophysical Research (Space Physics)*, *124*(8), 6613-6635. doi: 10.1029/2019JA026892

Solomon, S. C., Burns, A. G., Emery, B. A., Mlynczak, M. G., Qian, L., Wang, W., ... Wiltberger, M. (2012, August). Modeling studies of the impact of high-speed streams and co-rotating interaction regions on the thermosphere-ionosphere. *Journal of Geophysical Research (Space Physics)*, *117*, A00L11. doi: 10.1029/2011JA017417

Solomon, S. C., Qian, L., Didkovsky, L. V., Viereck, R. A., & Woods, T. N. (2011). Causes of low thermospheric density during the 2007 - 2009 solar minimum. *J. Geophys. Res.*, *116*. doi: 10.1029/2011JA016508

Strachan, L., Ko, Y. K., Panasyuk, A. V., Dobrzycka, D., Kohl, J. L., Romoli, M., ... Biesecker, D. A. (1999, January). Constraints on Coronal Outflow Velocities Derived from UVCS Doppler Dimming Measurements and in-Situ Charge State Data. , *87*, 311-314. doi: 10.1023/A:1005193711445

Strachan, L., Panasyuk, A. V., Dobrzycka, D., Kohl, J. L., Noci, G., Gibson, S. E., & Biesecker, D. A. (2000, February). Latitudinal dependence of outflow velocities from O VI Doppler dimming observations during the Whole Sun Month. , *105*(A2), 2345-2356. doi: 10.1029/1999JA900459

Temmer, M. (2021, December). Space weather: the solar perspective. *Living Reviews in Solar Physics*, *18*(1), 4. doi: 10.1007/s41116-021-00030-3

Thiemann, E. M. B., Eparvier, F. G., Bougher, S. W., Dominique, M., Andersson, L., Girazian, Z., ... Jakosky, B. M. (2018, September). Mars Thermospheric Variability Revealed by MAVEN EUVM Solar Occultations: Structure at Aphelion and Perihelion and Response to EUV Forcing. *Journal of Geophysical Research (Planets)*, *123*(9), 2248-2269. doi: 10.1029/2018JE005550

Thompson, B. J., Gibson, S. E., Schroeder, P. C., Webb, D. F., Arge, C. N., Bisi, M. M., ... Woods, T. N. (2011, December). A Snapshot of the Sun Near Solar Minimum: The Whole Heliosphere Interval. , *274*(1-2), 29-56. doi: 10.1007/s11207-011-9891-6

Torsti, J., Anttila, A., & Sahla, T. (1999). Concurrent solar and corotating interaction region particle events in august 1996. *Journal of Geophysical Research: Space Physics*, *104*(A5), 9891-9902. Retrieved from `https://agupubs.onlinelibrary.wiley.com/doi/abs/10.1029/1998JA900170` doi: https://doi.org/10.1029/1998JA900170

Torsti, J., Kocharov, L., Teittinen, M., Anttila, A., Laitinen, T., Makela, P., ... Valtonen, E. (1999). Energetic (10–65 mev) protons observed by erne on august 13–14, 1996: Eruption on the solar back side as a possible source of the event. *Journal of Geophysical Research: Space Physics*, *104*(A5), 9903-9909. Retrieved from `https://agupubs.onlinelibrary.wiley.com/doi/abs/10.1029/1998JA900017` doi: https://doi.org/10.1029/1998JA900017

Tsurutani, B. T., Gonzalez, W. D., Gonzalez, A. L. C., Guarnieri, F. L., Gopalswamy, N., Grande, M., ... Vasyliunas, V. (2006, July). Corotating solar wind streams and recurrent geomagnetic activity: A review. *Journal of Geophysical Research (Space Physics)*, *111*(A7), A07S01. doi: 10.1029/2005JA011273

Varela, J., Brun, A. S., Zarka, P., Strugarek, A., Pantellini, F., & Réville, V. (2022, November). MHD Study of Extreme Space Weather Conditions for Exoplanets With Earth-Like Magnetospheres: On Habitability Conditions and Radio-Emission. *Space Weather*, *20*(11), e2022SW003164. doi: 10.1029/2022SW003164

Vásquez, A. M., Huang, Z., Manchester, W. B., & Frazin, R. A. (2011, December). The WHI Corona from Differential Emission Measure Tomography. , *274*(1-2), 259-284. doi: 10.1007/s11207-010-9706-1

Vasyliunas, V. M. (1983). Physics of the Jovian magnetosphere. 11. Plasma distribution and flow. In *Physics of the jovian magnetosphere* (p. 395-453).

Vasyliunas, V. M. (1986, July). The convection-dominated magnetosphere of

Uranus. , *13*(7), 621-623. doi: 10.1029/GL013i007p00621

Verkhoglyadova, O. P., Tsurutani, B. T., Mannucci, A. J., Mlynczak, M. G., Hunt, L. A., Komjathy, A., & Runge, T. (2011, September). Ionospheric VTEC and thermospheric infrared emission dynamics during corotating interaction region and high-speed stream intervals at solar minimum: 25 March to 26 April 2008. *Journal of Geophysical Research (Space Physics)*, *116*(A9), A09325. doi: 10.1029/2011JA016604

Wang, W., Lei, J., Burns, A. G., Qian, L., Solomon, S. C., Wiltberger, M., & Xu, J. (2011, December). Ionospheric Day-to-Day Variability Around the Whole Heliosphere Interval in 2008. , *274*(1-2), 457-472. doi: 10.1007/s11207-011-9747-0

Wang, Y.-M., & Sheeley, N. R. J. (1990). Solar wind speed and coronal flux-tube expansion. *Astrophys. J.*, *355*, 726.

Wang, Y.-M., & Sheeley, N. R. J. (1991). Why fast solar wind originates from slowly expanding coronal flux tubes. *Astrophys. J. Lett.*, *372*, 45.

Warren, H. P., & Hassler, D. M. (1999). The density structure of a solar polar coronal hole. *Journal of Geophysical Research: Space Physics*, *104*(A5), 9781-9789. Retrieved from `https://agupubs.onlinelibrary.wiley.com/doi/abs/10.1029/1998JA900079` doi: https://doi.org/10.1029/1998JA900079

Webb, D. F., Cremades, H., Sterling, A. C., Mandrini, C. H., Dasso, S., Gibson, S. E., . . . Plunkett, S. P. (2011, December). The Global Context of Solar Activity During the Whole Heliosphere Interval Campaign. , *274*(1-2), 57-86. doi: 10.1007/s11207-011-9787-5

Webb, D. F., Gibson, S. E., Hewins, I. M., McFadden, R. H., Emery, B. A., Malanushenko, A., & Kuchar, T. (2018). Global solar magnetic field evolution over 4 solar cycles: Use of the mcintosh archive. *Frontiers in Astronomy and Space Sciences*.

Welsch, B. T., Christe, S., & McTiernan, J. M. (2011, December). Photospheric Magnetic Evolution in the WHI Active Regions. , *274*(1-2), 131-157. doi: 10.1007/s11207-011-9759-9

White, O., Kopp, G., Snow, M., & Tapping, K. (2011, December). The Solar Cycle 23 - 24 Minimum. A Benchmark in Solar Variability and Effects in the Heliosphere. , *274*(1-2), 159-162. doi: 10.1007/s11207-010-9680-7

Wijsen, N., Samara, E., Aran, À., Lario, D., Pomoell, J., & Poedts, S. (2021, February). A Self-consistent Simulation of Proton Acceleration and Transport Near a High-speed Solar Wind Stream. , *908*(2), L26. doi: 10.3847/2041-8213/abe1cb

Wiltberger, M., Qian, L., Huang, C.-L., Wang, W., Lopez, R. E., Burns, A. G., . . . Huang, Y. (2012, July). CMIT study of CR2060 and 2068 comparing L1 and MAS solar wind drivers. *Journal of Atmospheric and Solar-Terrestrial Physics*, *83*, 39-50. doi: 10.1016/j.jastp.2012.01.005

Wiltberger, M., Rigler, E. J., Merkin, V., & Lyon, J. G. (2017, March). Structure of High Latitude Currents in Magnetosphere-Ionosphere Models. , *206*(1-4), 575-598. doi: 10.1007/s11214-016-0271-2

Winslow, R. M., Lugaz, N., Philpott, L., Farrugia, C. J., Johnson, C. L., Anderson, B. J., . . . Asad, M. A. (2020, February). Observations of Extreme ICME Ram Pressure Compressing Mercury's Dayside Magnetosphere to the Surface. , *889*(2), 184. doi: 10.3847/1538-4357/ab6170

Witasse, O., Sánchez-Cano, B., Mays, M. L., Kajdič, P., Opgenoorth, H., Elliott, H. A., . . . Altobelli, N. (2017, August). Interplanetary coronal mass ejection observed at STEREO-A, Mars, comet 67P/Churyumov-Gerasimenko, Saturn, and New Horizons en route to Pluto: Comparison of its Forbush decreases at 1.4, 3.1, and 9.9 AU. *Journal of Geophysical Research (Space Physics)*, *122*(8), 7865-7890. doi: 10.1002/2017JA023884

Woods, T. N., Chamberlin, P. C., Harder, J. W., Hock, R. A., Snow, M., Eparvier,

F. G., ... Richard, E. C. (2009, January). Solar Irradiance Reference Spectra (SIRS) for the 2008 Whole Heliosphere Interval (WHI). , *36*(1), L01101. doi: 10.1029/2008GL036373

Woods, T. N., Harder, J. W., Kopp, G., & Snow, M. (2022, April). Solar-Cycle Variability Results from the Solar Radiation and Climate Experiment (SORCE) Mission. , *297*(4), 43. doi: 10.1007/s11207-022-01980-z

Younas, W., Khan, M., Amory-Mazaudier, C., & Amaechi, P. O. (2022, December). Ionospheric Response to the Coronal Hole Activity of August 2020: A Global Multi-Instrumental Overview. *Space Weather*, *20*(12), e2022SW003176. doi: 10.1029/2022SW003176

Zhao, L., & Fisk, L. (2011, December). Understanding the Behavior of the Heliospheric Magnetic Field and the Solar Wind During the Unusual Solar Minimum Between Cycles 23 and 24. , *274*(1-2), 379-397. doi: 10.1007/s11207-011-9840-4

Zhao, X. P., Hoeksema, J. T., & Scherrer, P. H. (1999). Changes of the boot-shaped coronal hole boundary during whole sun month near sunspot minimum. *Journal of Geophysical Research: Space Physics*, *104*(A5), 9735-9751. Retrieved from `https://agupubs.onlinelibrary.wiley.com/doi/abs/10.1029/1998JA900010` doi: https://doi.org/10.1029/1998JA900010

Zidowitz, S. (1999). Coronal structure of the whole sun month: A tomographic reconstruction. *Journal of Geophysical Research: Space Physics*, *104*(A5), 9727-9734. Retrieved from `https://agupubs.onlinelibrary.wiley.com/doi/abs/10.1029/1998JA900099` doi: https://doi.org/10.1029/1998JA900099